

Existence of singularly degenerate heteroclinic cycle in the Lorenz system and its dynamical consequences: Part I

Hiroshi Kokubu
Department of Mathematics
Kyoto University
Kyoto 606-8502, Japan
E-mail: kokubu@math.kyoto-u.ac.jp

Robert Roussarie
Institut de Mathématiques de Bourgogne
U.M.R. 5584 du CNRS
Université de Bourgogne
9, Avenue Alain Savary, B.P 47 870
21078 - Dijon Cedex, France
Email: roussari@u-bourgogne.fr

Dedicated to Prof. S.-N. Chow for his sixtieth birthday

June 16, 2004

Abstract

We prove that the Lorenz system with appropriate choice of parameter values has a specific type of heteroclinic cycle, called a singularly degenerate heteroclinic cycle, that consists of a line of equilibria together with a heteroclinic orbit connecting two of the equilibria. By an arbitrarily small but carefully chosen perturbation to the Lorenz system, we also show that the geometric model of Lorenz attractors formulated by Guckenheimer will bifurcate from it, among other things. Although not proven, one may also expect various other types of chaotic dynamics such as Hénon-like chaotic attractors, Lorenz attractors with hooks which were recently studied by S. Luzzatto and M. Viana, and what were observed in the original Lorenz system with large r and small b in the Sparrow's book [37]. Our analysis is all done within a family of three

dimensional ODEs that contains, as its subfamilies, the Lorenz system, the Rössler's second system and the Shimizu-Morioka system, which are known to exhibit Lorenz-like chaotic dynamics.

1 Introduction

In 1963, a meteorologist E. N. Lorenz [23] derived the following polynomial ordinary differential equations in the study of thermal fluid convection in relation to the question of long-term weather forecast:

$$\begin{aligned}\dot{x} &= \sigma(y - x) \\ \dot{y} &= rx - y - xz \\ \dot{z} &= -bz + xy.\end{aligned}\tag{1.1}$$

Setting the parameters (σ, r, b) to be at $(10, 28, 8/3)$, Lorenz numerically found a solution which remains bounded forever but behaves in a very complicated manner, as shown in Figure 1.

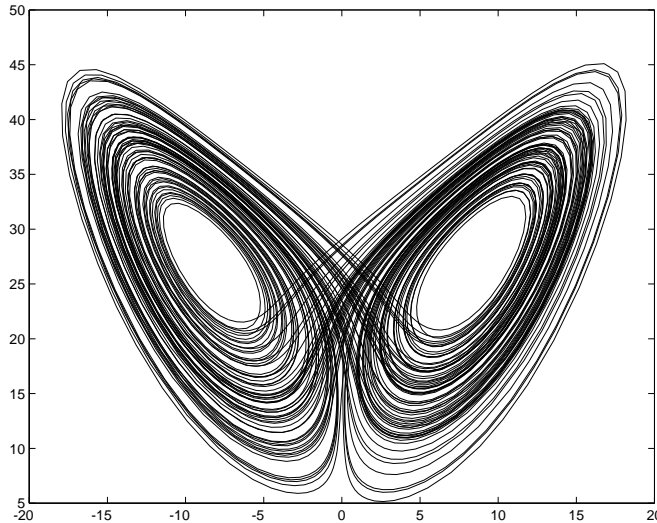


Figure 1: The “standard” Lorenz attractor.

This was one of the first examples of what is now known as “chaos”, and many papers have been devoted to study this seemingly chaotic dynamics of the Lorenz system, see e.g. [37] for relevant works by early 80’s, and [41] for a good updated review of developments of the study of the Lorenz system.

The first mathematically important contribution to understanding the above chaotic dynamics in (1.1) was made independently by Guckenheimer [14] (see also [16]), and Afraimovich, Bykov and Shil’nikov [1]. From the numerical simulation of (1.1), they have constructed a geometric model as an abstract three-dimensional vector field, and studied the dynamics of the chaotic attractor of the geometric model. Briefly they have proven the existence of a well-defined attractor in the geometric model, which is chaotic in the sense that the reduced interval mapping which carries essential dynamical information of the attractor is uniformly expanding, and such an attractor is, though not structurally stable, persistent under perturbation of the vector field.

Although it is constructed from the numerical simulation of the solution that exhibits a seemingly chaotic behavior, it was not at all clear whether the geometric model truly represents the dynamics in the Lorenz' original system, because rather strong hypotheses were imposed on the geometric model, that were not easily verified for (1.1).

Very recently, Tucker [39] gave a rigorous verification of the hypotheses for the geometric model in the Lorenz system at the standard parameter values $(\sigma, r, b) = (10, 28, 8/3)$. He used validated numerical integration of the Lorenz system (1.1) combined with a careful analysis near the equilibrium point where the orbits move very slowly and hence the numerical error bound cannot be effectively given. (Precisely speaking, the Poincaré map of the Lorenz system at the standard parameter values turns out not to be uniformly hyperbolic everywhere on the cross section. According to [39], several iterate of the Poincaré map does however become eventually hyperbolic, and hence the existence of the stable foliation is guaranteed.) Therefore the question of the existence of geometric Lorenz attractor in the original Lorenz system with the classical parameter values $\sigma = 10, r = 28, b = 8/3$ has been answered affirmatively by this computer assisted proof. Note also that, earlier to [39], Mischaikow, Mrozek and Szymczak [25], and independently Galias and Zgliczyński [13] gave a proof of the existence of chaotic dynamics in the Lorenz system (1.1) with classical and other parameter values in terms of semi-conjugacy to the symbolic dynamics. Although the method of [25, 13] is limited to detecting only symbolic dynamics and not a chaotic attractor, it is applicable to a broader class of systems at computationally lower cost.

In this paper, we shall furthermore investigate the Lorenz system and other relevant systems having similar behavior, hoping to give a better understanding of common features of Lorenz-like dynamics. The main results of this and a forthcoming paper may be summarized as follows:

Main Results

- (1) *The Lorenz system (1.1) with correctly chosen parameter values (σ, r, b) possesses a singularly degenerate heteroclinic cycle with arbitrarily large z -height.*
- (2) *Unfolding of the singularly degenerate heteroclinic cycle obtained as above can give rise to the geometric Lorenz attractor (and hopefully various other chaotic attractors that are observed in (1.1)).*
- (3) *In particular, a geometric Lorenz attractor exists in an arbitrarily small (but carefully chosen) perturbation of (1.1), although one may need to deviate from the original Lorenz system itself.*

Here the *singularly degenerate heteroclinic cycle* is an invariant set consisting of a line of equilibria and of a heteroclinic orbit connecting two equilibria in the line. In our case, the line of equilibria is the z -axis, one of these two equilibria is the origin, and the other is given by $P_* = (0, 0, G_*)$ for some large $G_* > 0$. The z -height of the cycle means the distance of the two equilibria measured along the z -axis, which is nothing but G_* for our case. See Figure 2. In order to have such a singularly degenerate heteroclinic cycle, we need to choose $b = 0$ in (1.1) so that the z -axis becomes the line of equilibria, and r sufficiently large, whereas $\sigma > 3/2$ remains bounded. As we will see in the proof, the equilibrium P_* has complex conjugate stable eigenvalues normal to the z -axis, that explains the spiral behavior of the singularly degenerate heteroclinic cycle near P_* as in Figure 2.

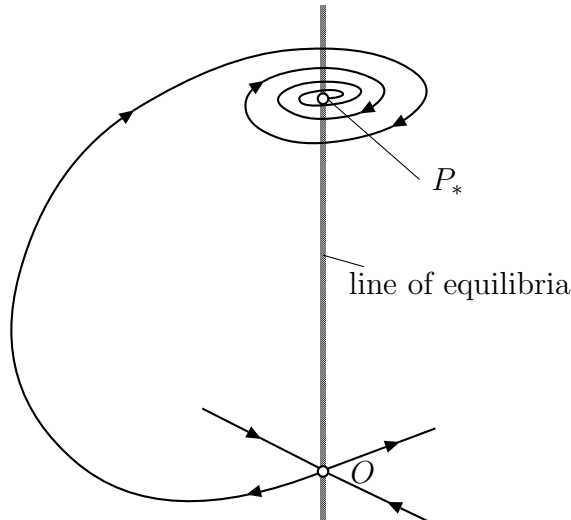


Figure 2: A singularly degenerate heteroclinic cycle.

Under such choice of parameters, we can then perturb (1.1) so that the perturbed vector field has an attractor in a small tubular neighborhood of the singularly degenerate heteroclinic cycle satisfying the hypotheses of the geometric model constructed by Guckenheimer and Williams [14], [16]. Note that the perturbation can be given by adding extra terms to (1.1) with arbitrarily small coefficients. As we shall discuss in later sections, we also expect that this singularly degenerate heteroclinic cycle can create other types of chaotic dynamics that are observed numerically in (1.1) and that are not explained by the geometric Lorenz attractor model.

The structure of the rest of this paper is as follows. In the next section, we shall give the precise statement of our results as well as further discussion on the motivation and relevant results. In §3 and §4, we give a proof of the existence of the singularly degenerate heteroclinic cycle. The main idea of the proof is the blow-up of the vector field at infinity. After the blow-up, we obtain a vector field on the sphere at infinity which has two equilibria, one at the north pole and another at the south pole, together with an orbit connecting these two equilibria. We then prove that such a connecting orbit persists in a neighborhood of the sphere at infinity. Since the equilibria at north and south poles are highly degenerate, we must blow-up again in order to carry out the analysis. Some Melnikov-like analysis, which is carried out in Appendix B, and a result in [12] will be used to complete the proof of the existence of the singularly degenerate heteroclinic cycle.

In the forthcoming Part II, we proceed to proving the existence of the geometric Lorenz attractor in a perturbed system. Here we briefly explain the contents of Part II. In §5, we shall make preliminary perturbation by introducing a movement on the z -axis by which the singularly degenerate heteroclinic cycle turns to a non-degenerate heteroclinic cycle where the line of equilibria changes to a heteroclinic orbit along the z -axis. We then study the Poincaré map along the non-degenerate heteroclinic cycle and its unfolding in §6, which is used in §7 to finish the proof of the existence of the geometric Lorenz attractors. The crucial points are the existence of an invariant

foliation for the Poincaré map that justifies the reduction to studying a one-dimensional interval map, and uniform expanding property of the one-dimensional map. For the former, we need to study the behavior of the vector field along the z -axis where the orbits still move slowly even after the perturbation, and hence the behavior in the normal direction should be taken into account. For the latter, we use a recent result of Oguro [26], which is given in Appendix C, for a new change of coordinates when the critical exponent is small. Recall that the critical exponent for the Lorenz attractor is given by the absolute value of the ratio of the unstable and weak stable eigenvalues, and it roughly gives the order of divergence of the derivative of the reduced one-dimensional map at the origin. For a typical form $x \mapsto \text{sign}(x)(c|x|^\omega - 1)$ of the map obtained in a usual context, it is assumed that the critical exponent ω is larger than $1/2$, thereby guaranteeing the uniform expansion in the one-dimensional map, see e.g. [32]. In our case, however, ω is close to 0, since our situation is a small perturbation from the singularly degenerate heteroclinic cycle. As a result the graph of our reduced one-dimensional map has very steep expanding part near the origin which quickly turns to an almost flat contracting part outside, hence seemingly no hope for the uniform expansion in this form. Oguro’s result says that, for such maps, if one can freely choose the coefficient c of the one-dimensional map, which is indeed the case in our setting by adjusting the unfolding parameters, there is a smooth change of coordinate by which the resulting map recovers the uniform expansion. Therefore, combining these results, we complete the proof of the existence of geometric Lorenz attractors in the unfolding of the heteroclinic cycle. §8 is the discussion section where we show other types of possible chaotic dynamics from the unfolding of our heteroclinic cycle and compare them with relevant known results.

This work was mainly done during the first author’s long-term visit to Laboratoire de Topologie, Université de Bourgogne in 2001. HK thanks the institute for its warm hospitality and the Monbu-Kagaku-sho grant for the financial support. HK was also partially supported by Grant-in-Aid for Scientific Research (No. 12440048,1434055), Ministry of Education, Science, Technology, Culture and Sports, Japan.

2 Motivation and statement of the main theorem

2.1 Motivation

The Lorenz system (1.1) has rich variety of chaotic dynamics of different kinds, and the chaotic attractor at the classical parameter values $(\sigma, r, b) = (10, 28, 8/3)$ which is modelled by the geometric Lorenz attractor is just one of them. For instance, [19] discusses a different type of chaotic dynamics in (1.1) for large r (around $r = 210$ while the other parameters are kept at the classical values) in which a numerically computed Poincaré map in a cross section gives rise to a folding map of a disk into itself. In fact, this chaotic attractor served as the origin of an equally famous chaotic attractor known as the Hénon attractor [18]. See Figure 3 for a computer generated attractor in the Lorenz system at $r = 210$. Furthermore, the dynamics of (1.1) in the case of large r and small b is numerically studied in detail in [37] where a new feature of behavior of orbits called “twisting around the z -axis” is observed. This gives an additional spiral motion

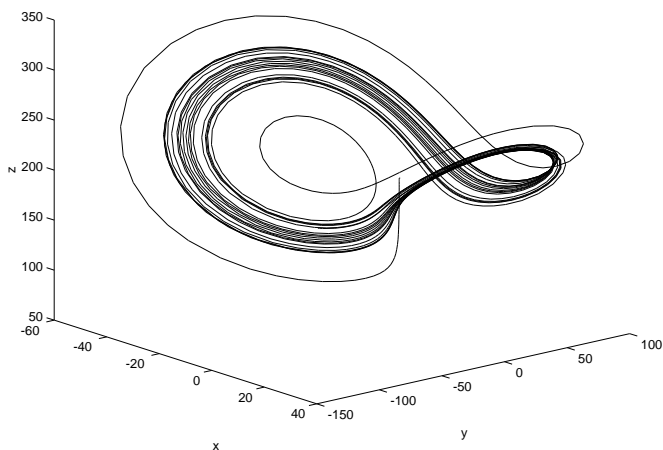


Figure 3: Chaotic attractor of the Lorenz system at $r = 210$, $b = 8/3$ and $\sigma = 10$.

around a part of the z -axis with large z values, and therefore the chaotic attractor in that parameter regime looks like the standard Lorenz attractor with an extra spiral behavior added on the top. See Figure 4.

Our principal motivation is to obtain good conceptual understanding of the essential structure of the Lorenz system which is responsible for creation of such a rich variety of dynamics. In other words, we want to find an organizing center, if any, for the dynamics in the Lorenz system.

On the other hand, there are other ordinary differential equations that exhibit chaotic dynamics similar to the Lorenz attractors. For instance, Rössler [29] gave the following system of ordinary differential equations:

$$\begin{aligned}\dot{x} &= x - xy - z \\ \dot{y} &= x^2 - ay \\ \dot{z} &= b(cx - z).\end{aligned}\tag{2.1}$$

This set of equations is different from his most famous one which is often called the Rössler's system, henceforth in this paper we call (2.1) the Rössler's second system. For the parameter values $(a, b, c) = (0.1, 0.08, 0.125)$, numerical simulation of this system shows chaotic dynamics as in Figure 5.

Another system exhibiting the Lorenz-like dynamics is the Shimizu-Morioka system [36]:

$$\begin{aligned}\dot{x} &= y \\ \dot{y} &= x(1 - z) - \lambda y \\ \dot{z} &= -\alpha z + x^2.\end{aligned}\tag{2.2}$$

Dynamics and bifurcations of this system are studied in [33] and [34], the latter of which discusses the relation to normal form containing (2.2) which shares a similar idea with the Lorenz-like system studied in this paper. In fact, it is clearly seen that the system (2.2) can be embedded into the system studied in this paper (2.4). See Appendix A for more discussion, in particular the relation to the results of [10].

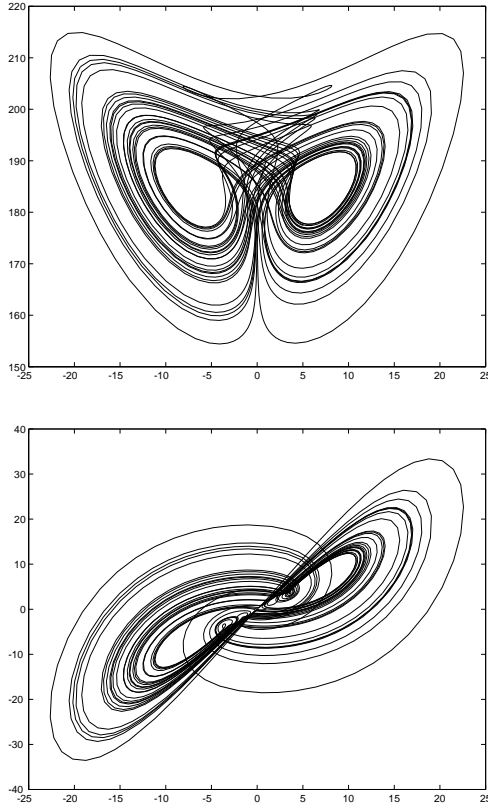


Figure 4: A chaotic attractor of Lorenz system (1.1) at $r = 185$.
Upper: (x, z) -plot; Lower: (x, y) -plot

As explained in Appendix A, the equations of these systems have some similarity and difference to the Lorenz system, and therefore it is not immediately seen the reason why numerically observed chaotic dynamics in these systems are similar (or somehow related) to the chaotic dynamics in the Lorenz system. To the best of our knowledge, there has been no serious attempt to study the Rössler's second system from mathematical point of view. However, see [40] for some hint of the relation.

Homoclinic orbits may be the first candidate for the organizing center of the Lorenz-like dynamics. It is numerically observed that the Lorenz system has (a symmetric pair of) homoclinic orbits associated to the origin when $\sigma = 10$, $b = 8/3$ and $r \approx 13.926\dots$. Moreover, Chen [6] gave a necessary and sufficient condition of the parameters (σ, b) for (1.1) to have a homoclinic orbit for some r . To be more explicit, he has proven that (1.1) has a homoclinic orbit to the origin for some $r > 0$ if and only if

$$\sigma > \frac{2b + 1}{3}.$$

Interestingly, one can see from his proof that the existing homoclinic orbit converges to a singularly degenerate heteroclinic cycle as $r \rightarrow \infty$ and $\sigma \rightarrow (2b + 1)/3$. Numerical experiments in [4] suggests that there are many different types of homoclinic orbits and many different homoclinic (or heteroclinic) bifurcations occurring in (1.1), and therefore it may be very natural to consider that some kind of homoclinic bifurcations

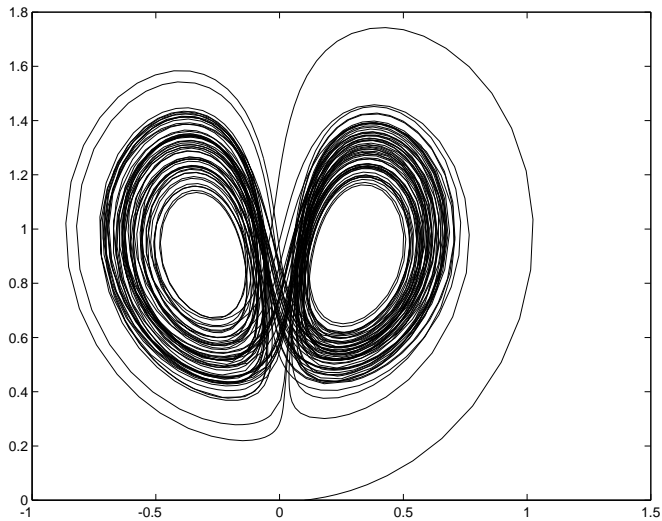


Figure 5: Chaotic attractor of the Rössler's second system. (x, y) -plot.

should be responsible for the Lorenz-like dynamics. See also [34] for similar numerically computed bifurcation sets of homoclinic orbits in the Shimizu-Morioka system (2.2).

Indeed, there have been several works devoted to the creation of the geometric Lorenz attractors via homoclinic bifurcations. The first result along this line was obtained by Rychlik [32], where he showed the bifurcation of the geometric Lorenz attractors from a symmetric pair of what is now called the inclination-flip homoclinic orbits. See e.g. [21] and [22] for the definition and related results about the inclination-flip homoclinic orbits. A part of the proof in [32] was postponed to the announced Part II which has unfortunately not appeared so far, but the readers may find it in a relevant work [11]. After [32], Robinson [28] also studied another type of homoclinic bifurcations creating geometric Lorenz attractors. These different homoclinic bifurcations are summarized in [27], in relation to other homoclinic bifurcations.

Not only the results of homoclinic bifurcations, these papers cited above also give concrete examples of polynomial ordinary differential equations which are proven to exhibit a geometric Lorenz attractor. We shall give only one example from [11] as this has, in our opinion, the closest form, among those examples, to the original Lorenz system:

$$\begin{aligned} \dot{x} &= y \\ \dot{y} &= Ax - By - xz - \gamma yz - x^3 \\ \dot{z} &= -\beta z + x^2. \end{aligned} \tag{2.3}$$

In [11] with slightly different notation, it is proven that, for appropriately chosen coefficients $A > 0$, $B > 0$, $\beta > 0$ and $\gamma < 0$ with $1/2 < \beta/\sqrt{A} < 1$, the corresponding system possesses a geometric Lorenz attractor. Indeed, the original Lorenz system and the Rössler's second system can be put into the above form by a suitable change of the space and time variables. See Appendix A for the explicit transformations.

Another interesting result was obtained in [2] where the authors studied a heteroclinic cycle involving a hyperbolic equilibrium point and a degenerate periodic orbit which is just at the moment of saddle-node bifurcation. This is a codimension one cycle (without symmetry) which is proven to produce a Lorenz-like attractor as formulated in [1]. This shares a common feature with our setting in the sense that there is a spiral

behavior in a part of the attractor.

Unfortunately, none of known bifurcation results for homoclinic and heteroclinic orbits seem to be applicable directly to the Lorenz and the Rössler's second systems, or even systems close to them. See also the discussion in Appendix A and in [11].

Hastings and Troy [17] used the so-called shooting method to show the existence of chaos in the Lorenz equations, with an aid of numerical computation. This is an analytical approach directly applied to the Lorenz equations, but the chaos proved there is a symbolic dynamics and not a chaotic attractor. Similar existence results of symbolic dynamics in the Lorenz equations at the classical parameter values were obtained by a topological approach combined with rigorous numerical computation by [25] and [13].

Idea of singular perturbation was used in Deng [8] for constructing Lorenz-like attractors in several concrete systems of ordinary differential equations. However, although the outlook of the attractors numerically obtained in such systems have some similarity to the chaotic attractor in the Lorenz equations, there is no proof or discussion about rigorous connection among those systems.

2.2 Statement of the main theorem

Now we give a precise statement of our main results:

Theorem 2.1

(1) Consider the system

$$\begin{aligned}\dot{x} &= y \\ \dot{y} &= Ax - By - xz - x^3 \\ \dot{z} &= -\beta z + x^2\end{aligned}\tag{2.4}$$

with $\beta = 0$. Then for any $B_* > 0$ which is smaller than some $B_0 \in (5/4, 2)$ and for sufficiently large $A_* > 0$, there exists $G_* = G_*(A_*, B_*)$ with $G_* = O(A_*)$ uniformly in B_* as $A_* \rightarrow \infty$, such that the system (2.4) with these parameter values possesses a singularly degenerate heteroclinic cycle connecting $O = (0, 0, 0)$ and $(0, 0, G_*)$.

(2) Consider perturbation of (2.4) in the following form:

$$\begin{aligned}\dot{x} &= y \\ \dot{y} &= Ax - By - xz - \gamma yz - x^3 - \eta xz^3 \\ \dot{z} &= -\beta z + x^2 + \delta z^2.\end{aligned}\tag{2.5}$$

Then, for any A close to A_* , B close to B_* , and γ, δ both positive and close to 0, there exist

$$G = G(A, B, \gamma, \delta) = G_* + O(|A - A_*| + |B - B_*| + |\gamma| + |\delta|)$$

and $\eta = o(|G|^{-1}) > 0$ such that the corresponding system (2.5) with these parameter values and with $\beta = \delta \cdot G$ possesses a (non-degenerate) heteroclinic cycle connecting $O = (0, 0, 0)$ and $(0, 0, G)$.

Moreover, an unfolding of the non-degenerate heteroclinic cycle gives rise to a geometric Lorenz attractor.

In Part I, we shall give a proof of the first assertion of this theorem, and the proof of second assertion is postponed to the forthcoming Part II. As is shown in Appendix A, the Lorenz system (1.1) can be transformed to the system (2.4). Moreover, by choosing $b = 0$ and r large enough in (1.1), while σ remains bounded, one can verify that the conditions of the first part of the above theorem are satisfied. Therefore the Lorenz system with such parameter values has a singularly degenerate heteroclinic cycle, as asserted in Main Results in Introduction. See Figure 6 for a numerically computed such cycle obtained in the original Lorenz system at a very large value of r and $b = 0$. For the third assertion of the Main Results in Introduction, one needs to leave the Lorenz system by adding the extra terms corresponding to γ, δ and η in (2.4), but it can be shown that these extra terms give only arbitrarily small (yet carefully chosen) perturbations to the original Lorenz system, hence the third assertion of Main Results also follows.

Remark 2.2 Similar results were obtained as in the following theorem for a system related to the Shimizu-Morioka system. See [10] and Appendix A for the details.

Theorem 2.3

(1) *Consider the system*

$$\begin{aligned}\dot{x} &= y \\ \dot{y} &= Ax - y - xz \\ \dot{z} &= -\beta z + x^2\end{aligned}\tag{2.6}$$

with $\beta = 0$. Then, for sufficiently large $A_ > 0$, there exists $G_* = G_*(A_*) = O(A_*)$ such that the system (2.6) with these parameter values possesses a singularly degenerate heteroclinic cycle connecting $O = (0, 0, 0)$ and $(0, 0, G_*)$.*

(2) *Consider perturbation of (2.6) as follows:*

$$\begin{aligned}\dot{x} &= y \\ \dot{y} &= Ax - y - xz - \gamma yz \\ \dot{z} &= -\beta z + x^2 + \delta z^2.\end{aligned}\tag{2.7}$$

Then, for any A close to A_ and γ, δ both positive and close to 0, there exists*

$$G = G(A, \gamma, \delta) = G_* + O(|A - A_*| + |\gamma| + |\delta|)$$

such that the corresponding system (2.7) with these parameter values and with $\beta = \delta \cdot G$ possesses a (non-degenerate) heteroclinic cycle connecting $O = (0, 0, 0)$ and $(0, 0, G)$.

Moreover, an unfolding of the non-degenerate heteroclinic cycle gives rise to a geometric Lorenz attractor.

At the end of this section, we want to make comparison of studies of dynamics for the Lorenz system and the Hénon family of diffeomorphisms in order to clarify the meaning of the results of this paper. It was numerically observed by Hénon [18] that the planar diffeomorphism given by

$$(x, y) \mapsto (y + 1 - ax^2, bx)\tag{2.8}$$

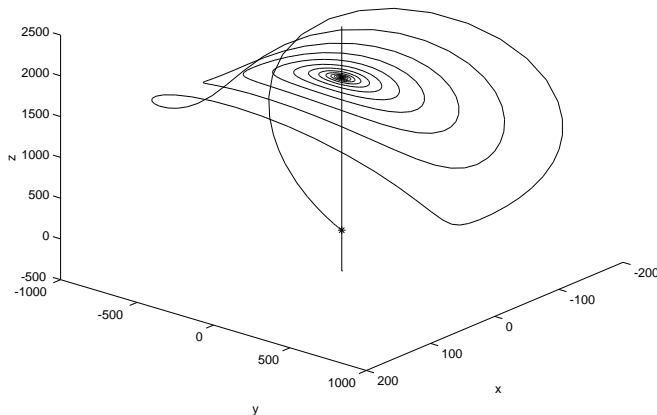


Figure 6: A singularly degenerate heteroclinic cycle in the Lorenz system, $r = 1000$, $b = 0$ and $\sigma = 10$.

exhibits a chaotic attractor when the parameters are chosen to be $a = 1.4$ and $b = 0.3$. However, up to now, there is no mathematically rigorous proof of the existence of such a chaotic attractors at the above classical parameter values. Much later, Benedicks and Carleson [3] proved the existence of non-trivial (non-uniformly hyperbolic) chaotic attractors in the Hénon map (2.8) with sufficiently small b and correctly chosen a from a set of positive Lebesgue measure. The key observation for their work was that when b is set to be 0, the Hénon map (2.8) reduces to the one-dimensional quadratic map $x \mapsto 1 - ax^2$, and hence for b close to 0, the Hénon map should be considered as a singular perturbation of the quadratic interval map. Since their proof strongly relies on the analysis of the quadratic map, it cannot be applied to the map with the classical parameter values $a = 1.4, b = 0.3$. However, the results indicate some hint of underlying mathematical structure of the Hénon map so that one might be convinced that the Hénon map with other parameter values could also have chaotic attractors of similar type, as observed by numerical simulation.

The history of the Lorenz system is somewhat different: After the numerical discovery of the chaotic attractor by [23], its geometric model was first constructed ([16], [1]) and studied intensively, from which a number of interesting dynamical consequences were obtained. Then the Lorenz system itself at the classical parameter values was investigated by Tucker [39] with the help of validated numerical computation, from which he successfully verified all the hypotheses needed to yield the previously obtained properties of the Lorenz system and its chaotic attractors.

Comparing these two streams of studies, one sees that what is missing in the Hénon map may be a good “geometric model” of the chaotic attractor, whereas in the Lorenz system, a “singular limit” from which generation of interesting chaotic dynamics can be conceptually understood. For the Hénon map, such a singular structure is rather clear from the expression of the map, whereas for the Lorenz system, it is not at all obvious what could be such a “singular limit”, because there is no clear singular structure seen from the expression. What we have shown in this paper is that such a possible “singular” and mathematically understandable structure may be obtained

once the system is transformed to the Lorenz-like system (2.4). Indeed, we believe that it would have been extremely hard to show the existence of singularly degenerate heteroclinic cycle if one studies the original system of the Lorenz equations.

In our case, we consider the extreme parameter values where $b = 0$ and $r \rightarrow \infty$ and find, in this extreme situation, a singular object, namely the singularly degenerate heteroclinic cycle in the Lorenz system. We unfold this very degenerate cycle to a usual heteroclinic cycle, then to a geometric Lorenz attractor. Since the singularly degenerate heteroclinic cycle is so degenerate, it has great potential of producing rich variety of dynamics. For instance, it agrees with the behavior of “twisting around the z -axis” observed in [37] for large r , and therefore it is intuitively close to the numerically observed chaotic attractor. This gives a hope that the singularly degenerate heteroclinic cycle may produce not only the geometric Lorenz attractors but also more variety of Lorenz-like chaotic dynamics including suspension of Hénon-like attractors [19]. We shall discuss this more in the last section. Finally, we emphasize that the results of [3] for the Hénon map are much stronger in the sense that they could understand the entire chaotic attractor of the Hénon map globally as long as their analysis works, whereas in our case the best we can do, at least at this moment, is to prove the existence of chaotic attractor in a small tubular neighborhood of the cycle.

Remark 2.4 Since it is necessary to choose γ close to 0 in the proof, and since the Rössler’s second system (2.1) is transformed into (2.5) with $\delta = \eta = 0$ but with $\gamma = 1$ which is not close to 0, our argument does not work for (2.1) as it is unfortunately. However, even in this case, some kind of singularly degenerate heteroclinic cycle is observed in a numerical simulation, and hence our point of view remains valid. We shall discuss this in more detail in §8.

Remark 2.5 One may notice that the inclusion of some of the terms in (2.5) is artificial; as we shall see later in the proof of the main theorem, the δz^2 term in the third line is used mainly to create an additional equilibrium on the z -axis which has no correspondence in the original Lorenz system (1.1), and the $\eta x z^3$ term in the second line is added in order to carry out some estimate for the perturbation. This may be true, but we do not know whether a similar result can be obtained for systems with no such artificial perturbation terms. We only point out that the term δz^2 appears naturally in normal form calculation which is closely related to the degenerate singularity related to Lorenz-like dynamics, see [10].

In the following sections, we shall give the proof of Theorem 2.1.

3 Blow-up at infinity (1): behavior on the sphere at infinity

In this and next sections, we give the existence of the singularly degenerate heteroclinic cycle in (2.4) with appropriate choice of parameters. More precisely, throughout these two sections, we mainly consider the following subfamily of (2.4) with $\beta = 0$:

$$\begin{aligned} \dot{x} &= y \\ \dot{y} &= Ax - By - xz - x^3 \\ \dot{z} &= x^2. \end{aligned} \tag{3.1}$$

We then shift the z -coordinate, namely introduce the change of coordinate $\tilde{z} = z - A$, which brings (3.1) to

$$\begin{aligned}\dot{x} &= y \\ \dot{y} &= -By - xz - x^3 \\ \dot{z} &= x^2,\end{aligned}\tag{3.2}$$

where z in fact stands for \tilde{z} , but we keep the same notation for simplicity. Observe that the z -axis is the line of equilibria in this system of equations.

The principal goal here is to find a singularly degenerate heteroclinic cycle in (3.2), which then shows the same conclusion in (3.1) by the reverse shift along the z -axis. Main idea to reach this goal is the method of blow-up. We shall carry out different blow-ups to (3.2); in this section, we shall apply what is called the blow-up at infinity, and in the next section, we then apply further blow-ups to the vector field obtained by the primary blow-up in this section in order to get more precise structure of the orbits. See e.g. [9] for more general account of the method of blow-ups in the study of dynamical systems.

3.1 First blow-up: the blow-up at infinity

The main idea of the blow-up at infinity is to compactify \mathbb{R}^3 to a 3-ball and, from the original vector field, define a vector field on the 3-ball, including the boundary sphere called the sphere at infinity, by introducing new coordinates which parametrize a family of curves emanating the origin and going off to infinity. To be more explicit, in order to compute the blow-up at infinity of (3.2), we use the following new coordinates:

$$x = \frac{u}{s}, \quad y = \frac{v}{s^2}, \quad z = \frac{w}{s},\tag{3.3}$$

where we consider (u, v, w) as coordinates on the unit 2-sphere, and s as the variable which parametrizes curves from the origin to infinity.

This choice of degrees 1, 2, 1 for s -variable is given by studying the quasi-homogeneity of terms in (3.2). Namely, if one wants to make

$$y \frac{\partial}{\partial x}, \quad x^3 \frac{\partial}{\partial y}, \quad x^2 \frac{\partial}{\partial z},$$

which are the highest order terms in each equation of (3.2), to be quasi-homogeneous, one must choose the quasi-homogeneous degree of x, y, z to be 1, 2, 1, respectively. See [9] for details of quasi-homogeneous blow-up technique. Another possibility may be to make

$$y \frac{\partial}{\partial x}, \quad xz \frac{\partial}{\partial y}, \quad x^2 \frac{\partial}{\partial z}$$

to be quasi-homogeneous, which results in choosing the quasi-homogeneous degree of x, y, z to be 3, 4, 5, respectively. But this turns out to be not so effective for the analysis of the blown-up vector fields. Therefore we have chosen (3.3) as the blow-up transformation.

The blown-up vector field by (3.3) can be given in several different charts: as we are interested in the behavior of vector field near infinity, we decompose a neighborhood of the sphere at infinity into three parts, namely

bottom chart: the chart given by $w = -1$ where we use (u, v, s) as the coordinates describing the vector field, with (u, v) in a compact disk around $(0, 0)$ of arbitrary radius;

top chart: the chart given by $w = +1$ where we use (u, v, s) as the coordinates with (u, v) in a compact disk around $(0, 0)$ of arbitrary radius;

side chart: after introducing the cylindrical coordinates (u, v, w) with $u = \rho \cos \theta$, $v = \rho \sin \theta$, the chart given by $\rho = 1$ where we use (w, θ, s) as the coordinates with w in a compact interval around 0 of arbitrary length.

Using the change of coordinates given above and the indicated local coordinates, the resulting blown-up vector fields in each chart of (3.2) are given as follows.

Lemma 3.1

(1) *The blow-up at infinity of (3.2) in the bottom chart is given by:*

$$\begin{aligned} s' &= su^2 \\ u' &= v + u^3 \\ v' &= -u^3 + 2u^2v - s(Bv - u). \end{aligned} \tag{3.4}$$

(2) *The blow-up at infinity of (3.2) in the top chart is given by:*

$$\begin{aligned} s' &= -su^2 \\ u' &= v - u^3 \\ v' &= -u^3 - 2u^2v - s(Bv + u). \end{aligned} \tag{3.5}$$

(3) *The blow-up at infinity of (3.2) in the side chart is given by:*

$$\begin{aligned} s' &= -s \cos \theta \sin^3 \theta + s^2(B \sin^2 \theta + w \sin \theta \cos \theta) \\ \theta' &= -(\cos^4 \theta + 2 \sin^2 \theta) - s(B \sin \theta \cos \theta + w \cos^2 \theta) \\ w' &= \cos^2 \theta(1 + \sin^2 \theta) - w \cos \theta \sin^3 \theta \\ &\quad + s(Bw \sin^2 \theta + w^2 \sin \theta \cos \theta). \end{aligned} \tag{3.6}$$

Note that in the above equations, the time derivative $'$ indicates that the time variable has also been changed accordingly, and the change may not be the same for all three results of blow-up. However, since the change of time variable is just given by multiplying an everywhere positive function, each of the vector field is equivalent to the original one, and hence there will be no problem in the following analysis.

The proof of lemma is a straightforward calculation, thus omitted.

3.2 Behavior on the sphere at infinity in the bottom and top charts

From (3.4), the blown-up vector field on the sphere at infinity in the bottom chart is given by setting $s = 0$, hence

$$\begin{aligned} u' &= v + u^3 \\ v' &= -u^3 + 2u^2v. \end{aligned}$$

This has a unique equilibrium at the origin which we call the south pole S for convenience of later use, which is globally repelling (i.e. globally attracting if the time

coordinate is reversed), because the Lie derivative of the function $\Phi(u, v) = u^4/2 + v^2$ with respect to the vector field is everywhere non-negative. Therefore any orbit on the sphere at infinity other than S must leave any compact domain of this chart in finite time.

Similarly in the top chart the blown-up vector field on the sphere at infinity

$$\begin{aligned} u' &= v - u^3 \\ v' &= -u^3 - 2u^2v \end{aligned}$$

has a unique equilibrium at the origin which we call the north pole N , which is globally attracting, because the same function $\Phi(u, v)$ has non-negative Lie derivative with respect to this vector field. Therefore any orbit that enters the top chart on the sphere converges to N as the time goes to ∞ .

Notice that the equilibria S and N in each of the local charts are highly degenerate, they are not structurally stable, and hence these behaviors on the sphere at infinity might be completely different from the behavior of nearby orbits close to but not on the sphere at infinity. We need more careful analysis for determining those orbits near the sphere at infinity, for which we use further blow-ups around S and N in the next section.

3.3 Behavior on the sphere at infinity in the side chart

The vector field on the sphere at infinity in the side chart is given by

$$\begin{aligned} \theta' &= -(\cos^4 \theta + 2 \sin^2 \theta) \\ w' &= \cos^2 \theta (1 + \sin^2 \theta) - w \cos \theta \sin^3 \theta, \end{aligned}$$

which is equivalent to

$$\frac{dw}{d\theta} = \frac{\cos \theta \sin^3 \theta}{\cos^4 \theta + 2 \sin^2 \theta} w - \frac{\cos^2 \theta (\cos^2 \theta + 2 \sin^2 \theta)}{\cos^4 \theta + 2 \sin^2 \theta}, \quad (3.7)$$

as the right hand side of the θ' -equation remains strictly negative.

Proposition 3.2 *The equation (3.7) has no periodic solution.*

Proof. The equation (3.7) is an inhomogeneous linear ordinary differential equation of the form $\frac{dw}{d\theta} = p(\theta)w - q(\theta)$, where

$$p(\theta) = \frac{\cos \theta \sin^3 \theta}{\cos^4 \theta + 2 \sin^2 \theta}, \quad q(\theta) = \frac{\cos^2 \theta (1 + \sin^2 \theta)}{\cos^4 \theta + 2 \sin^2 \theta}, \quad (3.8)$$

and therefore it can be solved by using the variation of constants formula:

$$w(\theta) = w(0) \exp \left(\int_0^\theta p(\sigma) d\sigma \right) - \int_0^\theta q(\varphi) \exp \left(\int_\varphi^\theta p(\sigma) d\sigma \right) d\varphi.$$

Observe that

$$\exp \int_0^\theta p(\sigma) d\sigma = (\cos^4 \theta + 2 \sin^2 \theta)^{1/4}. \quad (3.9)$$

Thus, by putting $\theta = 2\pi$, we obtain

$$w(2\pi) - w(0) = - \int_0^{2\pi} \frac{q(\varphi)}{(\cos^4 \varphi + 2 \sin^2 \varphi)^{1/4}} d\varphi,$$

which is strictly negative, since $q(\varphi) \geq 0$ which is not identically 0. Therefore the return map on the vertical axis $\{\theta = 0\}$ is a non-trivial translation. This proves the non-existence of periodic orbits in (3.7). \square

Combining all the above information, we can conclude that on the sphere at infinity, all the orbits except the equilibria S and N are connecting orbits between S and N ; any orbit other than S in the bottom chart must leave the bottom chart in finite time and enter the side chart where any orbit has monotone upward behavior, and therefore it eventually moves from the side chart into the top chart, hence converging to N .

In the next section, we shall study the vector fields near S and N in more detail using the second blow-ups, and prove that the orbits sufficiently close to the sphere at infinity behave similarly, hence proving the existence of the singularly degenerate heteroclinic cycle.

4 Blow-up at infinity (2): second blow-ups

In this section, we carry out the second blow-up for (3.4) and (3.5), and finish the proof of the existence of the singularly degenerate heteroclinic orbit.

4.1 Second blow-up for (3.4)

Recall (3.4) is given by

$$\begin{aligned} s' &= su^2 \\ u' &= v + u^3 \\ v' &= -u^3 + 2u^2v - s(Bv - u). \end{aligned}$$

Based on a similar reasoning for quasi-homogeneous degree of the variables, see Subsection 3.1, we blow-up this vector field with using the following rescaling:

$$s = r^2\Sigma, \quad u = rU, \quad v = r^2V,$$

and with two different charts as follows:

top chart: the chart given by $\Sigma = 1$ where we use (r, U, V) as the coordinates;

side chart: after introducing the cylindrical coordinates $U = R \cos \Theta$, $V = R \sin \Theta$, the chart given by $R = 1$ where we use (r, Θ, Σ) .

Note that we do not need to consider the bottom chart given by $\Sigma = -1$, because s being negative does not make sense. The next lemma can be proven by straightforward computation.

Lemma 4.1

(1) The blow-up of (3.4) in the top chart is given by:

$$\begin{aligned}\dot{r} &= \frac{1}{2}r^2U^2 \\ \dot{U} &= V + \frac{1}{2}rU^3 \\ \dot{V} &= U - U^3 + r(-BV + U^2V).\end{aligned}\tag{4.1}$$

(2) The blow-up of (3.4) in the side chart is given by:

$$\begin{aligned}\dot{r} &= r(\cos\Theta\sin^3\Theta + \Sigma\cos\Theta\sin\Theta) \\ &\quad + r^2(\cos^4\Theta + 2\cos^2\Theta\sin^2\Theta - B\Sigma\sin^2\Theta) \\ \dot{\Theta} &= -(\cos^4\Theta + 2\sin^2\Theta) + \Sigma\cos^2\Theta \\ &\quad - Br\Sigma\cos\Theta\sin\Theta \\ \dot{\Sigma} &= -2\Sigma(\cos\Theta\sin^3\Theta + \Sigma\cos\Theta\sin\Theta) \\ &\quad - r\Sigma(\cos^4\Theta + 2\cos^2\Theta\sin^2\Theta - 2B\Sigma\sin^2\Theta).\end{aligned}\tag{4.2}$$

In particular, the planes given by $r = 0$ and by $\Sigma = 0$ are both invariant under the blown-up vector field.

4.2 Analysis of (4.1)

The vector field (4.1) restricted to the (U, V) -plane is a Hamiltonian system with the Hamiltonian function

$$H(U, V) = \frac{1}{2}V^2 + \frac{1}{4}U^4 - \frac{1}{2}U^2,\tag{4.3}$$

and in particular, there are three equilibrium points, one at the origin which is a saddle, and two others at $(U, V) = (\pm 1, 0)$ which are centers. There is also a pair of symmetric homoclinic orbits to the origin. Away from the (U, V) -plane, the r -axis is a line of equilibria, which is normally hyperbolic, at least for small $r > 0$, and hence we can speak about its stable and unstable manifolds. In particular, we are interested in the structure of the unstable manifold of the r -axis. Let $W^u(r)$ denote the unstable manifold of the equilibrium $(0, 0, r)$ for sufficiently small $r > 0$. Our goal is the next proposition.

Proposition 4.2 *There exists $B_0 \in (5/4, 2)$ such that for any $0 < B < B_0$, for any large $L > 0$, for any small $\delta > 0$, and for any sufficiently small $r > 0$, the unstable manifold $W^u(r)$ must leave the domain $\{U^2 + V^2 \leq L\} \times [0, \delta]$ in finite time, and does so from its side boundary $\{U^2 + V^2 = L\}$.*

This means that the unstable manifold of $(0, 0, r)$ with sufficiently small $r > 0$ remains sufficiently close to the (U, V) -plane until its projection to the plane leaves any compact domain (and hence the top chart). Since this orbit is very close to the Hamiltonian vector field

$$\begin{aligned}\dot{U} &= V \\ \dot{V} &= U - U^3,\end{aligned}\tag{4.4}$$

it spirals around the r -axis many times before leaving the top chart, although the r -axis is normally of saddle-type.

In order to prove the above proposition, we make use of the fact that the vector field for small r is close to the Hamiltonian vector field (4.4), and apply the so-called Melnikov analysis. Let P denote (U, V) and consider the solution

$$P(t; U_0, r_0) = (U(t; U_0, r_0), V(t; U_0, r_0)) \quad \text{and} \quad r(t; U_0, r_0)$$

of (4.1) with the initial condition at $t = 0$ given by $P = (U, V) = (U_0, 0)$ ($U_0 \geq \sqrt{2}$) and $r = r_0 > 0$. Let $T(U_0, r_0)$ be the time $t > 0$ at which the solution satisfies

$$V(t; U_0, r_0) = 0, \quad \frac{dV}{dt}(t; U_0, r_0) < 0$$

for the first time. This is well-defined for small enough r_0 , since the orbit behave close to that of (4.4). Define

$$\eta(U_0, r_0) = H(P(T(U_0, r_0); U_0, r_0)), \quad \rho(U_0, r_0) = r(T(U_0, r_0); U_0, r_0).$$

Lemma 4.3 *The functions $\eta(U_0, r_0)$ and $\rho(U_0, r_0)$ have the following asymptotic expansions as $r_0 \rightarrow 0$:*

$$\eta(U_0, r_0) = h_0 - \left(\int_{\Gamma_{h_0}} \gamma \right) r_0 + O(r_0^2), \quad (4.5)$$

$$\rho(U_0, r_0) = r_0 + \frac{1}{2} \left(\oint U_{h_0}(t)^2 dt \right) r_0^2 + O(r_0^3), \quad (4.6)$$

where $h_0 = H(U_0, 0)$, Γ_{h_0} is a closed curve given by $H(U, V) = h_0$, $U_{h_0}(t)$ is the U -component of the solution of the (4.4) with the initial condition $(U_0, 0)$, and γ is a 1-form given by

$$\gamma = \frac{1}{2} U^3 dV + (B - U^2) V dU.$$

Notice that when $h_0 = 0$ (and hence $U_0 = \sqrt{2}$), $\Gamma_{h_0=0}$ degenerates to the homoclinic figure eight curve, but for $h_0 > 0$, Γ_{h_0} remains to be a regular periodic orbit.

Proof. The first term Taylor expansion of the function $\eta(U_0, r_0)$ with respect to r_0 at $r_0 = 0$ is

$$\eta(U_0, 0) = H(P(T(U_0, 0); U_0, 0)) = H(U_0, 0) = h_0,$$

since $P(t; U_0, 0)$ is simply a solution of (4.4).

The coefficient of the second term of the Taylor expansion is

$$\frac{\partial \eta}{\partial r_0}(U_0, 0) = \frac{dH}{dt} \cdot \frac{\partial T}{\partial r_0} + \nabla H \cdot \frac{\partial P}{\partial r_0},$$

but the conservation of the Hamiltonian implies

$$\frac{dH}{dt}(T) \Big|_{r_0=0} = \frac{dH}{dt}(T(U_0, 0); U_0, 0) = 0,$$

and hence we obtain

$$\frac{\partial \eta}{\partial r_0}(U_0, 0) = \nabla H(P(T; U_0, 0)) \cdot \frac{\partial P}{\partial r_0}(T; U_0, 0).$$

Since $\frac{\partial P}{\partial r_0}(t)|_{r_0=0} = (U_{r_0}(t), V_{r_0}(t))$ is a solution of (part of) the variational equation to (4.1), namely

$$\begin{aligned} \dot{U}_{r_0} &= V_{r_0} + \frac{1}{2} U^3 \\ \dot{V}_{r_0} &= (1 - 3U^2) U_{r_0} + (-BV + U^2 V), \end{aligned}$$

we get

$$\begin{aligned}
\frac{d}{dt} \left(\nabla H \cdot \frac{\partial P}{\partial r_0} \right) &= \frac{d}{dt} (H_U \cdot U_{r_0} + H_V \cdot V_{r_0}) \\
&= (3U^2 - 1)\dot{U} \cdot U_{r_0} + (U^3 - U) \cdot \dot{U}_{r_0} \\
&\quad + \dot{V} \cdot V_{r_0} + V \cdot \dot{V}_{r_0} \\
&= \frac{1}{2}(U^3 - U)U^3 + V(-BV + U^2V) \\
&= -\frac{1}{2}U^3 \cdot \dot{V} - (B - U^2)V \cdot \dot{U}.
\end{aligned}$$

On the other hand, $(U_{r_0}(0), V_{r_0}(0)) = (0, 0)$ at $t = 0$, and hence $(\nabla H \cdot \frac{\partial P}{\partial r_0})(0) = 0$. Therefore we obtain

$$\begin{aligned}
\frac{\partial \eta}{\partial r_0}(U_0, 0) &= (\nabla H \cdot \frac{\partial P}{\partial r_0})(T) \\
&= - \int_{H(U,V)=h_0} \frac{1}{2}U^3 dV + (B - U^2)V dU \\
&= - \int_{\Gamma_{h_0}} \gamma,
\end{aligned}$$

which proves (4.5).

We proceed to the Taylor expansion of $\rho(U_0, r_0)$ with respect to r_0 at $r_0 = 0$. Since the plane given by $r = 0$ is invariant, clearly $\rho(U_0, 0) = 0$. Moreover, from the form of the \dot{r} -equation in (4.1), $r(t; U_0, 0) \equiv 0$ for any t , and hence

$$\frac{d}{dt} \frac{\partial r}{\partial r_0} = rU^2 \cdot \frac{\partial r}{\partial r_0} = 0,$$

which yields $\frac{\partial r}{\partial r_0}(T) = \frac{\partial r}{\partial r_0}(0) = 1$. Therefore we obtain

$$\frac{\partial \rho}{\partial r_0}(U_0, 0) = \dot{r} \cdot \frac{\partial T}{\partial r_0} + \frac{\partial r}{\partial r_0}(T) = 1.$$

This gives the second term of the Taylor expansion of $\rho(U_0, r_0)$.

Similarly, using the above information, the first three terms of the right hand side of

$$\frac{\partial^2 \rho}{\partial r_0^2}(U_0, 0) = \ddot{r} \cdot \left(\frac{\partial T}{\partial r_0} \right)^2 + \dot{r} \cdot \frac{\partial^2 T}{\partial r_0^2} + 2 \frac{d}{dt} \frac{\partial r}{\partial r_0} + \frac{\partial^2 r}{\partial r_0^2}(T)$$

vanish, and from the \dot{r} -equation of (4.1),

$$\left. \frac{d}{dt} \frac{\partial^2 r}{\partial r_0^2} \right|_{r_0=0} = \left. \left(\frac{\partial r}{\partial r_0} \right)^2 \right|_{r_0=0} U^2 = U^2,$$

thus we obtain

$$\frac{\partial^2 \rho}{\partial r_0^2}(U_0, 0) = \frac{\partial^2 r}{\partial r_0^2}(T) = \oint U_{h_0}^2 dt,$$

hence (4.6). This completes the proof of the lemma. \square

Since the integral

$$\int_{\Gamma_{h_0}} \gamma = \int_{H(U,V)=h_0} \frac{1}{2} U^3 dV + (B - U^2) V dU$$

is nothing but a Melnikov-type integral, and we want to know the behavior of the value of this integral with respect to h_0 , we follow the conventional notation for the Melnikov analysis as follows. We solve the equation $H(U, V) = \frac{1}{2}(V^2 + \frac{1}{2}U^4 - U^2) = h_0$ with respect to V as $V = \sqrt{2h_0 + U^2 - \frac{1}{2}U^4}$ and define a function $M(h_0)$ as

$$M(h_0) = \frac{1}{4} \int_{\Gamma_{h_0}} \gamma = \int_0^{U_0} \left(\frac{1}{2} U^3 \frac{dV}{dU} + (B - U^2) V \right) dU.$$

We claim that this function always takes negative value. More precisely,

Proposition 4.4 *There exists $B_0 \in (5/4, 2)$ such that, for any $0 < B < B_0$, the Melnikov integral $M(h_0)$ satisfies*

$$\forall h_0 \geq 0, \quad M(h_0) \leq M_0 < 0$$

for some $M_0 < 0$ that is independent of $h_0 \geq 0$.

Recall that the Hamiltonian value $h_0 = 0$ corresponds to the homoclinic orbits in (4.4).

Since the proof of this proposition is rather lengthy and will not be used in later analysis, we give it in Appendix B, and now we proceed to the proof of Proposition 4.2 using Proposition 4.4.

For convenience, we abuse the notation and from now on consider $(\eta(U_0, r_0), \rho(U_0, r_0))$ as a mapping Φ acting on the (h_0, r_0) -plane, namely

$$\begin{aligned} \Phi(h_0, r_0) &= (\eta(h_0, r_0), \rho(h_0, r_0)) && (h_0, r_0 \geq 0) \\ &= (h_0 - 4M(h_0)r_0 + O(r_0^2), r_0 + K(h_0)r_0^2 + O(r_0^3)), \end{aligned}$$

where $K(h_0)$ is the coefficient of r_0^2 in (4.6). This makes sense, because U_0 and h_0 are related as $H(U_0, 0) = h_0$, and they are in one to one correspondence at least in the range $h_0 \geq 0$ and $U_0 \geq \sqrt{2}$. Therefore we shall regard $\Phi(h_0, r_0)$ as having the asymptotic expansion given in Lemma 4.3. Our goal is to give estimates of the iterates of this mapping Φ with an initial point (h_0, r_0) for sufficiently small $r_0 > 0$. consider the h -component.

Lemma 4.5 *There exists $\bar{h} > 0$ such that, for sufficiently small $r_0 > 0$, the h -component of the solution starting $(0, r_0)$ must reach \bar{h} in finite time, and the r -component of the solution grows only less than $2r_0$ during that time.*

Proof. First we make initial choice of $\bar{h} > 0$ and $\bar{r} > 0$ small enough so that

$$\rho(h_0, r_0) < C$$

is satisfied for some (large) $C > 0$ as long as $0 \leq h_0 \leq \bar{h}$ and $0 \leq r_0 \leq \bar{r}$. Under this circumstance, the evolution of the r -component of the iterates of Φ is dominated by the solution of the differential inequality

$$\frac{dr}{dt} \leq Ar^2$$

for some $A > 0$. Notice that the function $K(h_0)$ remains bounded even at $h_0 = 0$, because $U_{h_0}(t)$ for $h_0 = 0$ is a homoclinic solution to a hyperbolic equilibrium, and therefore has exponential decay as $t \rightarrow \infty$, which guarantees the convergence of the integral defining $K(0)$, and hence the existence of A .

By choosing \bar{h} smaller if necessary, we may assume $\bar{h} < |M_0|/A$. Also, by choosing \bar{r} smaller if necessary, we have $\eta(h_0, r_0) - h_0 > 2|M_0|r_0$ for any h_0 . Here we have used the fact that the r -component of the iterates $\Phi^i(h_0, r_0)$ is no less than r_0 , which follows from $\rho(U, r) \geq r$ for any (U, r) in a domain where (4.6) is valid. Therefore if we choose $N_* = 1/(2Ar_0)$, then, for any $N \geq N_*$, the h -component of the N -th iterate of Φ is larger than

$$2|M_0|r_0 \times N > \frac{|M_0|}{A} > \bar{h},$$

thus we obtain the desired conclusion for the h -component. (Note that one can choose A suitably so that N_* becomes an integer.) During this time, the growth of the r -component is estimated by solving the above differential inequality, hence we obtain

$$r\text{-component of } \Phi^N(0, r_0) \leq \frac{r_0}{1 - Ar_0N} \leq \frac{r_0}{1 - Ar_0/(2Ar_0)} = 2r_0$$

for $N \leq N_*$. Therefore the claim follows. \square

Now we consider the growth of the iterates of Φ in the range $\bar{h} \leq h \leq L$ for arbitrary $L > 0$.

Lemma 4.6 *For any large $L > 0$ and for any small $\delta > 0$, there exists $r_* > 0$ such that the h -component of the iterates of Φ starting (\bar{h}, r_*) must reach L while the r -component remains less than δ .*

Clearly Proposition 4.2 follows once the above lemma is proven, for which, we need the following:

Lemma 4.7 *For any $h_* \in [\bar{h}, L]$, there exists $\alpha, \beta > 0$, with β arbitrarily small, such that in the domain $D_* = [h_* - \alpha, h_* + \alpha] \times [0, \beta]$, there are sets W_\pm , where W_- is a half open outer neighborhood of a bottom part of the left vertical edge of D_* and W_+ is a half open inner neighborhood of the (entire) right vertical boundary of edge, satisfying that any orbit of the iterates of Φ leaving W_- must immediately enters D_* and leaves D_* in finite number of iterates necessarily through W_+ . See Figure 7.*

Proof. From the form of Φ :

$$(h_0, r_0) \mapsto (h_0 - 4M(h_0)r_0 + O(r_0^2), r_0 + K(h_0)r_0^2 + O(r_0^3)),$$

we can apply the results of [12] and conclude that Φ is C^∞ -conjugate to the time 1 map of the vector field

$$\begin{aligned} \dot{h} &= r \cdot [-4M(h) + O(r)] \\ \dot{r} &= r^2 \cdot [K(h) + O(r)], \end{aligned}$$

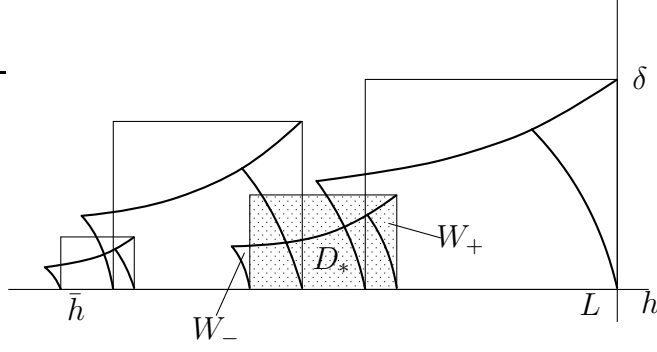


Figure 7: Sets W_{\pm} in Lemma 4.7

which is equivalent, by time reparametrization, to

$$\begin{aligned} h' &= -4M(h) + O(r) \\ r' &= r[K(h) + O(r)]. \end{aligned}$$

Since $M(h) \neq 0$ for any $h \in [0, \infty)$, the latter vector field is non-singular in a small enough neighborhood of the line $r = 0$ and the line $r = 0$ itself is invariant. Therefore, there exists a flow-box in a neighborhood of $(h_*, 0)$ that contains a segment in $r = 0$. The construction of W_{\pm} is now straightforward from this fact. \square

Proof of Lemma 4.6. For any $h_* \in [\bar{h}, L]$, we can choose D_* that satisfies the assertion of Lemma 4.7. Since the segment $[\bar{h}, L]$ is compact, only finitely many such D_* can cover the whole segment $[\bar{h}, L]$. By connecting orbits using the corresponding W_{\pm} for these finitely many D_* 's, we can obtain the desired orbit remaining in an arbitrary small rectangular neighborhood of the segment $[\bar{h}, L]$ and travels from its left vertical edge to the right vertical edge.

This completes the proof of Lemma 4.6, and thus Proposition 4.2. \square

4.3 Analysis of (4.2)

In the previous subsection, we have shown that the unstable manifold $W^u(r)$ of an equilibrium point $(0, 0, r)$ for sufficiently small $r > 0$ leaves the top chart of the second blow-up of (3.4) in finite time, and enters the side chart where the orbits are governed by the equation (4.2):

$$\begin{aligned} \dot{r} &= r (\cos \Theta \sin^3 \Theta + \Sigma \cos \Theta \sin \Theta) \\ &\quad + r^2 (\cos^4 \Theta + 2 \cos^2 \Theta \sin^2 \Theta - B \Sigma \sin^2 \Theta) \\ \dot{\Theta} &= -(\cos^4 \Theta + 2 \sin^2 \Theta) + \Sigma \cos^2 \Theta \\ &\quad - Br \Sigma \cos \Theta \sin \Theta \\ \dot{\Sigma} &= -2 \Sigma (\cos \Theta \sin^3 \Theta + \Sigma \cos \Theta \sin \Theta) \\ &\quad - r \Sigma (\cos^4 \Theta + 2 \cos^2 \Theta \sin^2 \Theta - 2B \Sigma \sin^2 \Theta). \end{aligned}$$

Here we prove that $W^u(r)$ passes through and leaves the side chart in finite time, thereby proving that it indeed leaves the bottom chart of the first blow-up. Once we

have shown this assertion, we can conclude that $W^u(r)$ must enter within finite time the top chart of the first blow-up, since, as we have already seen in the previous section, the behavior of orbits in the side chart of the first blow-up are regular on the sphere at infinity and hence in its neighborhood as well.

In order to verify that $W^u(r)$ from the top chart of the second blow-up must leave the side chart of the second blow-up in finite time, we again use the results of [12]. Observe from (4.2) that, when $\Sigma = 0$, $\dot{\Theta} = -(\cos^4 \Theta + 2 \sin^2 \Theta) \leq -1$, and hence the return map with respect to the (r, Σ) coordinates is well-defined. More explicitly, consider the differential equations:

$$\begin{aligned} \frac{dr}{d\Theta} &= -\frac{\cos \Theta \sin \Theta (\sin^2 \Theta + \Sigma) + O(r)}{\cos^4 \Theta + 2 \sin^2 \Theta + \Sigma \cos^2 \Theta + O(r)} \cdot r \\ \frac{d\Sigma}{d\Theta} &= \frac{2 \cos \Theta \sin \Theta (\sin^2 \Theta + \Sigma) + O(r)}{\cos^4 \Theta + 2 \sin^2 \Theta + \Sigma \cos^2 \Theta + O(r)} \cdot \Sigma, \end{aligned} \quad (4.7)$$

which are obtained by taking the ratios of the right hand sides of (4.2). For an initial condition (r_0, Σ_0) at $\Theta = 0$, let $(r(\Theta; r_0, \Sigma_0), \Sigma(\Theta; r_0, \Sigma_0))$ be the solution of the above equations. Then we can define the return map $(R(r_0, \Sigma_0), S(r_0, \Sigma_0))$ as

$$R(r_0, \Sigma_0) = r(-2\pi; r_0, \Sigma_0), \quad S(r_0, \Sigma_0) = \Sigma(-2\pi; r_0, \Sigma_0).$$

Note that, since $\dot{\Theta} < 0$, Θ decreases as the time variable of (4.2) increases, hence taking values at $\Theta = -2\pi$ in the above definition. This return map clearly leave both the Σ - and r -axes invariant, since so is (4.2).

Lemma 4.8 *The return map $(r_0, \Sigma_0) \mapsto (R(r_0, \Sigma_0), S(r_0, \Sigma_0))$ satisfies the following:*

$$\begin{aligned} R(r_0, \Sigma_0) &= r_0 + r_0^2 [R_* + O(|r_0| + |\Sigma_0|)] \\ S(r_0, \Sigma_0) &= \Sigma_0 + r_0 \Sigma_0 [S_* + O(|r_0| + |\Sigma_0|)], \end{aligned}$$

for some $R_* > 0$ and $S_* < 0$.

Proof. First observe that, from the invariance of the r - and Σ -axes, the solution of (4.7) satisfies

$$r(\Theta; 0, \Sigma_0) \equiv 0, \quad \Sigma(\Theta; r_0, 0) \equiv 0,$$

that implies $R(0, \Sigma_0) \equiv 0$, $S(r_0, 0) \equiv 0$. This means R is divisible by r_0 and S by Σ_0 , hence

$$R(r_0, \Sigma_0) = r_0 \tilde{R}(r_0, \Sigma_0), \quad S(r_0, \Sigma_0) = \Sigma_0 \tilde{S}(r_0, \Sigma_0),$$

for some \tilde{R}, \tilde{S} , for which we claim that they can be written as:

$$\tilde{R}(r_0, \Sigma_0) = 1 + r_0 \hat{R}(r_0, \Sigma_0), \quad (4.8)$$

$$\tilde{S}(r_0, \Sigma_0) = 1 + r_0 \hat{S}(r_0, \Sigma_0), \quad (4.9)$$

for some \hat{R}, \hat{S} , and that

$$\begin{aligned} R_* &= \hat{R}(0, 0) = \frac{\partial \tilde{R}}{\partial r_0}(0, 0) = \frac{1}{2} \frac{\partial^2 R}{\partial r_0^2}(0, 0) > 0, \\ S_* &= \hat{S}(0, 0) = \frac{\partial \tilde{S}}{\partial r_0}(0, 0) = \frac{\partial^2 S}{\partial r_0 \partial \Sigma_0}(0, 0) < 0. \end{aligned}$$

Once these are proven, we obtain the desired conclusion

$$\begin{aligned}\tilde{R}(r_0, \Sigma_0) &= 1 + r_0[R_* + O(|r_0| + |\Sigma_0|)], \\ \tilde{S}(r_0, \Sigma_0) &= 1 + r_0[S_* + O(|r_0| + |\Sigma_0|)].\end{aligned}$$

Differentiating the first equation of (4.7) with respect to r_0 and evaluating it at $r_0 = 0$, we obtain

$$\frac{d}{d\Theta} \left(\frac{\partial r}{\partial r_0} \Big|_{r_0=0} \right) = - \frac{\cos \Theta \sin^3 \Theta + \Sigma(\Theta) \cos \Theta \sin \Theta}{\cos^4 \Theta + 2 \sin^2 \Theta - \Sigma(\Theta) \cos^2 \Theta} \cdot \frac{dr}{dr_0} \Big|_{r_0=0},$$

and hence it can be solved as

$$\frac{\partial r}{\partial r_0}(\Theta; 0, \Sigma_0) = \frac{\partial r}{\partial r_0}(0; 0, \Sigma_0) \cdot \exp \left(\int_0^\Theta A(\varphi) d\varphi \right),$$

where $A(\Theta)$ is the coefficient of the above linear differential equation. Notice that, from the form of the Hamiltonian vector field given by (4.3) in the top chart, the solution $\Sigma(\Theta) = \Sigma(\Theta; 0, \Sigma_0)$ can be taken as a π -periodic even function by shifting the parametrization of Θ , if necessary. This implies

$$\int_0^{-2\pi} A(\varphi) d\varphi = 0,$$

from which and $\frac{\partial r}{\partial r_0}(0; 0, \Sigma_0) \equiv 1$, we obtain

$$\tilde{R}(0, \Sigma_0) = \frac{\partial r}{\partial r_0}(-2\pi; 0, \Sigma_0) \equiv 1,$$

hence proving (4.8).

For (4.9), we first observe that the return map restricted to the Σ -axis is the identity map, namely $S(0, \Sigma_0) = \Sigma_0$, again due to the fact that the vector field given by the blow-up locus in the top chart is Hamiltonian, hence completely integrable. This implies that $S(r_0, \Sigma_0) - \Sigma_0$ is divisible by r_0 , and therefore we can write

$$S(r_0, \Sigma_0) = \Sigma_0 + r_0 \check{S}(r_0, \Sigma_0).$$

On the other hand, $S(r_0, \Sigma_0)$ is divisible by Σ_0 , hence so is $\check{S}(r_0, \Sigma_0)$, from which we have (4.9).

In order to evaluate the constants R_* and S_* , we use the differential equations for $\frac{\partial^2 r}{\partial r_0^2}$ and $\frac{\partial \check{\Sigma}}{\partial r_0}$. A straightforward computation gives that they satisfy:

$$\begin{aligned}\frac{d}{d\Theta} \frac{\partial^2 r}{\partial r_0^2}(\Theta; 0, 0) &= -p(\Theta) \frac{\partial^2 r}{\partial r_0^2}(\Theta; 0, 0) - 2q(\Theta) \\ \frac{d}{d\Theta} \frac{\partial \check{\Sigma}}{\partial r_0}(\Theta; 0, 0) &= 2p(\Theta) \frac{\partial \check{\Sigma}}{\partial r_0}(\Theta; 0, 0) + q(\Theta),\end{aligned}$$

where p and q are given by (3.8). From (3.9), we can use the variation of constants formula to explicitly solve the above differential equations and obtain

$$\begin{aligned}R_* = \frac{1}{2} \frac{\partial^2 r}{\partial r_0^2}(-2\pi; 0, 0) &= - \int_0^{-2\pi} q(\Theta) \exp \left(\int_\Theta^{-2\pi} -p(\varphi) d\varphi \right) d\Theta \\ &= \int_0^{2\pi} q(\Theta) \exp \left(\int_\Theta^{2\pi} -p(\varphi) d\varphi \right) d\Theta,\end{aligned}$$

and

$$\begin{aligned} S_* &= \frac{\partial \tilde{\Sigma}}{\partial r_0}(-2\pi; 0, 0) = \int_0^{-2\pi} q(\Theta) \exp\left(\int_{\Theta}^{-2\pi} 2p(\varphi) d\varphi\right) d\Theta \\ &= -\int_0^{2\pi} q(\Theta) \exp\left(\int_{\Theta}^{2\pi} 2p(\varphi) d\varphi\right) d\Theta. \end{aligned}$$

Clearly from the form of the integrals, R_* is a positive number and S_* is a negative number. Approximate values given by numerical evaluation of these integrals using Maple are

$$R_* \approx 3.577 > 0, \quad \text{and} \quad S_* \approx -3.305 < 0.$$

This completes the proof of the lemma. \square

Due to [12], Lemma 4.8 implies that the return map $(R(r_0, \Sigma_0), S(r_0, \Sigma_0))$ is C^∞ -conjugate to the time one map of a vector field of the form

$$\begin{aligned} \dot{r} &= r^2[R_* + O(|r| + |\Sigma|)] \\ \dot{\Sigma} &= r\Sigma[S_* + O(|r| + |\Sigma|)], \end{aligned}$$

which is equivalent by time reparametrization to

$$\begin{aligned} r' &= r[R_* + O(|r| + |\Sigma|)] \\ \Sigma' &= \Sigma[S_* + O(|r| + |\Sigma|)]. \end{aligned}$$

Since this last vector field has a hyperbolic saddle equilibrium at the origin, and since both the Σ - and r -axes are invariant, we obtain the desired conclusion. Notice also that $r \mapsto r^\omega$ is the leading term of the transition map of orbits passing near the saddle, with the ratio of the stable and unstable eigenvalues of the saddle to the above vector field being $\omega = -S_*/R_* \approx 0.92396$. This will be used later to obtain the asymptotic behavior of $W^u(r)$.

4.4 Second blow-up for (3.5)

We proceed in the same way to the analysis of (3.5):

$$\begin{aligned} s' &= -su^2 \\ u' &= v - u^3 \\ v' &= -u^3 - 2u^2v - s(Bv + u), \end{aligned}$$

namely we make further blow-up of (3.5) and prove that $W^u(r)$ which is proven to enter the top chart where (3.5) is defined, really converges to a single equilibrium on the line of equilibria. Once this is proven, it will complete the proof of the existence of a singularly degenerate heteroclinic orbit by blow-down the vector field.

As before, we blow-up (3.5) using the following rescaling:

$$s = r^2\Sigma, \quad u = rU, \quad v = r^2V,$$

and with the same two different charts:

top chart: the chart given by $\Sigma = 1$ where we use (r, U, V) as the coordinates;

side chart: after introducing the cylindrical coordinates $U = R \cos \Theta$, $V = R \sin \Theta$, the chart given by $R = 1$ where we use (r, Θ, Σ) .

Lemma 4.9

(1) *The blow-up of (3.5) in the top chart is given by:*

$$\begin{aligned} \dot{r} &= -\frac{1}{2}r^2U^2 \\ \dot{U} &= V - \frac{1}{2}rU^3 \\ \dot{V} &= -U - U^3 - r(BV + U^2V). \end{aligned} \tag{4.10}$$

(2) *The blow-up of (3.4) in the side chart is given by:*

$$\begin{aligned} \dot{r} &= r \left(\cos \Theta \sin^3 \Theta - \Sigma \cos \Theta \sin \Theta \right. \\ &\quad \left. - r^2 (\cos^4 \Theta + 2 \cos^2 \Theta \sin^2 \Theta + B \Sigma \sin^2 \Theta) \right) \\ \dot{\Theta} &= - \left(\cos^4 \Theta + 2 \sin^2 \Theta + \Sigma \cos^2 \Theta \right) \\ &\quad - Br \Sigma \cos \Theta \sin \Theta \\ \dot{\Sigma} &= -2 \Sigma \left(\cos \Theta \sin^3 \Theta - \Sigma \cos \Theta \sin \Theta \right) \\ &\quad + r \Sigma \left(\cos^4 \Theta + 2 \cos^2 \Theta \sin^2 \Theta + 2B \Sigma \sin^2 \Theta \right). \end{aligned} \tag{4.11}$$

In particular, the planes given by $r = 0$ and by $\Sigma = 0$ are both invariant under the blown-up vector field.

4.5 Analysis of (4.11)

Here we also proceed exactly the same way as in the analysis of (4.2). If one views the right hand side of (4.2) and (4.11) as polynomials in terms of r and Σ with coefficients being functions of Θ , then the difference of (4.2) and (4.11) are only in the signs of some of the terms. Therefore we can obtain the same form of expression of the return map

$$(r_0, \Sigma_0) \mapsto (\bar{R}(r_0, \Sigma_0), \bar{S}(r_0, \Sigma_0))$$

as

$$\begin{aligned} \bar{R}(r_0, \Sigma_0) &= r_0 + r_0^2[\bar{R}_* + O(|r_0| + |\Sigma_0|)] \\ \bar{S}(r_0, \Sigma_0) &= \Sigma_0 + r_0 \Sigma_0[\bar{S}_* + O(|r_0| + |\Sigma_0|)], \end{aligned}$$

and only difference here is that

$$\bar{R}_* = -R_* \approx -3.577 < 0, \quad \bar{S}_* = -S_* \approx 3.305 > 0.$$

This suffices to conclude that the orbit of $W^u(r)$ coming into the side chart of the second blow-up of (3.5) must leave it in finite time and enters the top chart. Moreover, the leading term of the transition map near the saddle in this side chart is given by $r \mapsto r^{\bar{\omega}}$, where $\bar{\omega} = -R_*/S_* = 1/\omega$, which compensates the asymptotic behavior obtained at the end of §4.3.

4.6 Analysis of (4.10)

Finally we come to the last part and study (4.10). This vector field restricted to the (U, V) -plane is again a Hamiltonian system whose Hamiltonian function is given by

$$H(U, V) = \frac{1}{2}V^2 + \frac{1}{4}U^4 + \frac{1}{2}U^2,$$

and in particular, there is a unique equilibrium at the origin which is a global center for this planar system. Our goal is to show that each orbit which is close to the (U, V) -plane must be attracted to a single equilibrium on the line of equilibria at the r -axis. The main idea is again the results of [12].

First we make change of coordinates $(U, V) = (\rho \cos \varphi, \rho \sin \varphi)$, which brings (4.10) into

$$\begin{aligned}\dot{\varphi} &= -1 - \rho^2 \cos^4 \varphi - r\rho(B \cos \varphi \sin \varphi + \frac{1}{2}\rho^2 \cos^3 \varphi \sin \varphi) \\ \dot{\rho} &= -\rho^3 \cos^3 \varphi \sin \varphi + r\rho(B \sin \varphi - \frac{1}{2}\rho^2 \cos^4 \varphi - \rho^2 \cos^2 \sin^2 \varphi) \\ \dot{r} &= -\frac{1}{2}r^2 \rho^2 \cos^2 \varphi.\end{aligned}$$

In the same way as in the analysis of (4.2) and (4.11), we observe that for small enough r , the right hand side of the $\dot{\varphi}$ -equation is strictly negative, hence it is possible to regard (r, ρ) as functions of φ which satisfy the differential equations:

$$\frac{dr}{d\varphi} = -\frac{\frac{1}{2}r^2 \rho^2 \cos^2 \varphi}{1 + \rho^2 \cos^4 \varphi + O(r\rho)} \quad (4.12)$$

$$\frac{d\rho}{d\varphi} = \frac{\rho^3 \cos^3 \varphi \sin \varphi + r\rho B \sin \varphi + O(r\rho^3)}{1 + \rho^2 \cos^4 \varphi + O(r\rho)}. \quad (4.13)$$

Solutions of these differential equations define the return map

$$(r_0, \rho_0) \mapsto (R(r_0, \rho_0), T(r_0, \rho_0)), \quad (4.14)$$

where

$$R(r_0, \rho_0) = r(-2\pi; r_0, \rho_0), \quad T(r_0, \rho_0) = \rho(-2\pi; r_0, \rho_0).$$

Proposition 4.10 *The return map (4.14) has the following asymptotic expansion:*

$$\begin{aligned}R(r_0, \rho_0) &= r_0 + r_0^2 \rho_0^2 \left(-\frac{3\pi}{8} + \dots\right) \\ T(r_0, \rho_0) &= \rho_0 + r_0 \rho_0^2 \left(-\pi + \dots\right).\end{aligned}$$

Once this is proven, we can again use the result of [12]. In fact, since $(R(r_0, \rho_0) - r_0, T(r_0, \rho_0) - \rho_0)$ are factored out by $r_0 \rho_0$, we can say that this return map is C^∞ -conjugate to the time 1 map of the vector field

$$\begin{aligned}\dot{r} &= \rho \left(-\frac{3\pi}{8}r + \dots\right) \\ \dot{\rho} &= -\pi\rho + \dots\end{aligned}$$

This vector field clearly shows that the r -axis is normally hyperbolic and attracting, and hence $W^u(r)$ finally converges to some equilibrium $(0, 0, \bar{r})$ in this chart. Therefore we obtain the desired conclusion.

Furthermore, since the ratios of the eigenvalues of the saddles in each of the side charts of the second blow-ups (4.2) and (4.11) are mutually inverse of the other, as remarked above, and since the average in θ of the first equation of (3.6) gives 0 as its coefficient of the leading term with respect to s at $s = 0$, the correspondence between $r > 0$ in the top chart of the second blow-up of (3.4) and its limiting equilibrium $(0, 0, \bar{r})$ are asymptotically equivalent as $r \rightarrow 0$. This shows that, going back to the original coordinates of (3.2) after blow-down, the two equilibria $(0, 0, -A)$ and $(0, 0, \bar{A})$, $A, \bar{A} > 0$, that are connected by the heteroclinic orbit, are related as $\bar{A} = O(A)$

as $A \rightarrow \infty$. Therefore, if we choose such a sufficiently large singularly degenerate heteroclinic cycle in (3.2) and let $-A_*$ be given by the z -coordinate of the bottom equilibrium of the heteroclinic orbit, then the shifted heteroclinic orbit by $z \mapsto z + A_*$ in (3.1) connects the origin and an equilibrium $(0, 0, G_*)$ with

$$G_* = A_* + \bar{A}_* \quad \text{with} \quad G_* = O(A_*) \text{ as } A_* \rightarrow \infty. \quad (4.15)$$

So what remains is the proof of the above proposition, which is given below.

Proof of Proposition 4.10 and completion of the proof of Theorem 2.1(1). Observe first that

$$r(\varphi; 0, \rho_0) \equiv 0, \quad \rho(\varphi; r_0, 0) \equiv 0,$$

which follow from the invariance of the plane given by $r = 0$ and the cylinder given by $\rho = 0$. From the latter, we have

$$\frac{dr}{d\varphi}(\varphi; r_0, 0) \equiv 0,$$

and hence $r(\varphi; r_0, 0) \equiv r_0$, namely

$$R(r_0, 0) \equiv r_0.$$

Also notice that when $r = 0$, the system (4.10) defines a Hamiltonian vector field on the (U, V) -plane whose orbits are all periodic orbits surrounding the origin. Therefore, the solution $\rho(\varphi; 0, \rho_0)$ is 2π -periodic in φ and, by shifting the parametrization, it can be considered as an even function of φ . In particular, we have

$$T(0, \rho) \equiv \rho_0.$$

From these identities, we can expand $R(r_0, \rho_0)$ and $T(r_0, \rho_0)$ as follows:

$$\begin{aligned} R(r_0, \rho_0) &= r_0 + r_0 \rho_0 \bar{R}(r_0, \rho_0) \\ T(r_0, \rho_0) &= \rho_0 + r_0 \rho_0 \bar{T}(r_0, \rho_0). \end{aligned}$$

For this form, we claim the following:

- (a) $\bar{T}(r_0, 0) \equiv 0$,
- (b) $\bar{R}(r_0, 0) \equiv 0$,
- (c) $\bar{R}(0, \rho_0) \equiv 0$,
- (d) $\frac{\partial^3 \rho}{\partial r_0 \partial \rho_0^2}(-2\pi; 0, 0) = -2\pi$,
- (e) $\frac{\partial^4 r}{\partial r_0^2 \partial \rho_0^2}(-2\pi; 0, 0) = -\frac{3\pi}{2}$.

The first claim (a) shows $\bar{T}(r_0, \rho_0)$ is divisible by ρ_0 and (b) and (c) show that $\bar{R}(r_0, \rho_0)$ is divisible by $r_0 \rho_0$. Then (d) and (e) give the coefficients of the leading terms of the expansion of $\bar{R}(r_0, \rho_0)$ and $\bar{T}(r_0, \rho_0)$, which all together prove the desired assertion of the proposition.

The first three claims can be proven similarly, so we shall only give a proof of the claim (a). From the definition of $\bar{T}(r_0, \rho_0)$, one has

$$\frac{\partial T}{\partial \rho_0}(r_0, 0) = 1 + r_0 \bar{T}(r_0, 0).$$

Differentiating (4.13) with respect to ρ_0 and evaluating it at $\rho_0 = 0$, we obtain

$$\frac{d}{d\varphi} \left(\frac{\partial \rho}{\partial \rho_0} \right) \Big|_{\rho_0=0} = Br_0 \sin \varphi \cdot \left(\frac{\partial \rho}{\partial \rho_0} \right) \Big|_{\rho_0=0},$$

hence $\frac{\partial \rho}{\partial \rho_0}(\varphi; r_0, 0)$ is 2π -periodic in φ . This shows that

$$\frac{\partial T}{\partial \rho_0}(r_0, 0) = \frac{\partial \rho}{\partial \rho_0}(-2\pi; r_0, 0) = \frac{\partial \rho}{\partial \rho_0}(0; r_0, 0) = 1,$$

from which we get $\bar{T}(r_0, 0) \equiv 0$. The proof of the claims (b) and (c) are similar, hence left to the readers.

The evaluation of the derivatives in the claims (d) and (e) can be done by very tedious but straightforward computation using the differential equations (4.12) and (4.13), hence we omit it. This completes the proof of Proposition 4.10.

Combining all these results of analysis, we have completed the proof of the first assertion of Theorem 2.1. \square

Remark 4.11 Those who are familiar with the blow-up method for vector fields might ask if there may be a different scaling for the first blow-up at infinity that simplifies the proof. In fact, if we take a slightly different scaling

$$x = \frac{u}{s}, \quad y = \frac{v}{s^2}, \quad z = \frac{w}{s^2},$$

for the blow-up at infinity of (3.2), then we obtain the same vector fields as (4.1) and (4.10) in the bottom and top charts. However, the equation for the side chart becomes different, and seems more difficult to study the dynamics than (3.6), therefore we finally decided to proceed in the way given in this and previous sections.

A Coordinate transformations to the Lorenz-like system

Lorenz system

The Lorenz system (1.1)

$$\begin{aligned} \dot{x} &= \sigma(y - x) \\ \dot{y} &= rx - y - xz \\ \dot{z} &= -bz + xy \end{aligned}$$

can be transformed, by the coordinate change

$$X = px, \quad Y = q(y - x), \quad Z = m(z - \ell x^2), \quad \tau = kt, \quad (\text{A.1})$$

with

$$p = \frac{1}{\sqrt{2}(2\sigma - b)}, \quad \sqrt{2}q = \frac{\sigma}{(2\sigma - b)^2} = m, \quad \ell = \frac{1}{2\sigma}, \quad k = 2\sigma - b,$$

to a subfamily of the system (2.4):

$$\begin{aligned} X' &= Y \\ Y' &= AX - BY - XZ - X^3 \\ Z' &= -\beta Z + X^2 \end{aligned} \quad (' = \frac{d}{d\tau})$$

with

$$A = \frac{\sigma(r-1)}{(2\sigma-b)^2}, \quad B = \frac{\sigma+1}{2\sigma-b}, \quad \beta = \frac{b}{2\sigma-b}. \quad (\text{A.2})$$

Notice that the relation given by (A.2) between (A, B, β) and (r, σ, b) is a diffeomorphic change of parameters in reasonable domains of definition including the case discussed in this paper when A being very large, β being very small and B remaining bounded around 1. Having this in mind, we can transform (2.5) with non-zero but small γ and δ by the inverse of (A.1), assuming (A, B, β) are given by (A.2), and we obtain

$$\begin{aligned} \dot{x} &= \sigma(y-x) \\ \dot{y} &= rx - y - xz - \frac{\sigma\gamma}{2\sigma-b}yz - \frac{\gamma}{2(2\sigma-b)}(x^3 - x^2y) \\ \dot{z} &= -bz + xy + \delta(2\sigma-b) \left(z - \frac{x^2}{2\sigma} \right)^2. \end{aligned}$$

Therefore, if γ and δ are small, we can see that the system (2.5) can be considered a small perturbation of the original Lorenz system.

Rössler's second system

By the coordinate change

$$X = px, \quad Y = q(x - xy - z), \quad Z = my, \quad \tau = kt$$

with

$$p = m = \frac{1}{k} = \frac{1}{b-a}, \quad q = \frac{1}{(b-a)^2},$$

the Rössler's second system (2.1)

$$\begin{aligned} \dot{x} &= x - xy - z \\ \dot{y} &= x^2 - ay \\ \dot{z} &= b(cx - z) \end{aligned}$$

is transformed to

$$\begin{aligned} X' &= Y \\ Y' &= AX - BY - XZ - \gamma YZ - X^3 \\ Z' &= -\beta Z + X^2 + \delta Z^2 \end{aligned} \quad (' = \frac{d}{d\tau})$$

with

$$A = \frac{b(1-c)}{(b-a)^2}, \quad B = \frac{b-1}{b-a}, \quad \beta = \frac{a}{b-a}, \quad \gamma = 1, \quad \delta = 0.$$

Unfolding of a nilpotent singularity with \mathbb{Z}_2 -symmetry

[10] carried out the study of the normal form and its unfolding of a nilpotent singularity with a non-degenerate 2-jet of vector fields on \mathbb{R}^3 having a reflectional symmetry with respect to a line, and in particular, the following vector field was analysed:

$$\begin{aligned}\dot{x} &= y \\ \dot{y} &= \lambda x + \mu y - xz + byz + \text{h.o.t.} \\ \dot{z} &= \nu + x^2 + z^2 + \text{h.o.t.}\end{aligned}$$

After a suitable rescaling, the above family can be brought to

$$\begin{aligned}X' &= Y \\ Y' &= \bar{\lambda}X + \bar{\mu}Y - XZ + (\text{small terms}) \\ Z' &= X^2 + (\text{small terms})\end{aligned} \quad (' = \frac{d}{d\tau}),$$

and the existence of a singularly degenerate heteroclinic cycle was proven for the family with the small terms truncated. The argument of §5 and §6 in this paper applies to this family with small terms, and thus the geometric Lorenz attractor exists in the above family, and hence in the unfolding of the nilpotent singularity of codimension three as claimed in [10].

Shimizu-Morioka system

The Shimizu-Morioka system (2.2)

$$\begin{aligned}\dot{x} &= y \\ \dot{y} &= x(1-z) - \lambda y \\ \dot{z} &= -\alpha z + x^2\end{aligned}$$

can be directly embedded to the system (2.4). However, by making additional rescaling

$$x = \lambda^2 X, \quad y = \lambda^3 Y, \quad z = \lambda^2 Z, \quad \tau = \lambda t,$$

we obtain

$$\begin{aligned}X' &= Y \\ Y' &= \frac{1}{\lambda^2}X - Y - XZ \\ Z' &= -\frac{\alpha}{\lambda^2}Z + X^2\end{aligned} \quad (' = \frac{d}{d\tau}).$$

When $\alpha = 0$ and λ is small, this is the same situation studied in [10] discussed above, for which a singularly degenerate heteroclinic cycle is shown to exist. Therefore we can prove that a singularly degenerate heteroclinic cycle also exists in the Shimizu-Morioka system, and that, by a similar reasoning given in this paper, the geometric Lorenz attractor is generated by an arbitrarily small (but correctly chosen) perturbation of the Shimizu-Morioka system.

B Melnikov analysis

In this section, we shall give a proof of Proposition 4.4 using the standard technique which can be found in e.g. [5].

Let $c(h)$ be a unique solution $U = c(h)$ of the equation $H(U, 0) = h$ for a given h , and define

$$J_i(h) = \int_0^{c(h)} U^{2i} V dU \quad (i = 0, 1, 2),$$

where V is related to U, h through $H(U, V) = h$, namely $V = V(U, h) = \sqrt{2h + U^2 - U^4/2}$, and in particular, $V(c(h), h) \equiv 0$. From

$$\frac{dJ_i(h)}{dh} = \int_0^{c(h)} \frac{U^{2i}}{V} dU, \quad (\text{B.1})$$

it is possible to express

$$\begin{aligned} M(h) &= \int_0^{c(h)} \left\{ \frac{1}{2} U^3 dV + (B - U^2) V dU \right\} \\ &= \int_0^{c(h)} \left\{ \frac{1}{2} U^3 \left(\frac{U - U^3}{V} \right) + (B - U^2) V \right\} dU \end{aligned} \quad (\text{B.2})$$

in terms of J_i and its derivatives. For this purpose, we shall first derive some properties of the functions J_i .

By straightforward evaluation of integrals using $c(0) = \sqrt{2}$, we obtain

Lemma B.1

$$J_0(0) = \frac{2}{3}, \quad J_1(0) = \frac{8}{15}.$$

Lemma B.2 *The functions J_0 and J_1 satisfy the differential equations:*

$$\frac{d}{dh} \begin{pmatrix} J_0 \\ J_1 \end{pmatrix} = \frac{1}{4h(4h+1)} \begin{pmatrix} 4(3h+1) & -1 \\ -4h & 4h \end{pmatrix} \begin{pmatrix} J_0 \\ 5J_1 \end{pmatrix}.$$

Proof. From (B.1), we have

$$\begin{aligned} J_0 &= \int_0^{c(h)} \frac{V^2}{V} dU = \int_0^{c(h)} \frac{2h + U^2 - U^4/2}{V} dU \\ &= 2h \left(\frac{dJ_0}{dh} \right) + \left(\frac{dJ_1}{dh} \right) - \frac{1}{2} \left(\frac{dJ_2}{dh} \right). \end{aligned}$$

On the other hand, using integration by parts and implicit differentiation, as get

$$\begin{aligned} J_0 &= [UV]_0^{c(h)} - \int_0^{c(h)} U \frac{dV}{dU} dU = - \int_0^{c(h)} \frac{U^2 - U^4}{V} dU \\ &= - \left(\frac{dJ_1}{dh} \right) + \left(\frac{dJ_2}{dh} \right). \end{aligned}$$

By eliminating dJ_2/dh from these two, we obtain

$$3J_0 = 4h \left(\frac{dJ_0}{dh} \right) + \left(\frac{dJ_1}{dh} \right).$$

Similarly for J_1 , we get

$$5J_1 = \frac{4h}{3} \left(\frac{dJ_0}{dh} \right) + \frac{4(3h+1)}{3} \left(\frac{dJ_1}{dh} \right),$$

and, together with these two equations, we obtain the desired conclusion. \square

Let $\Phi(h) = \frac{J_1(h)}{J_0(h)}$. From Lemma B.1, we have $\Phi(0) = \frac{4}{5}$.

Lemma B.3

$$M(h) = \frac{1}{2}J_0(h) \cdot (2B - 5\Phi(h)).$$

Proof. From (B.2), $V^2 = 2h + U^2 - U^4/2$ and Lemma B.2, we have

$$\begin{aligned} M(h) &= \int_0^{c(h)} \left\{ \frac{1}{2}U^3(U - U^3) + (B - U^2) \left(2h + U^2 - \frac{U^4}{2} \right) \right\} \frac{dU}{V} \\ &= 2Bh \left(\frac{dJ_0}{dh} \right) + (B - 2h) \left(\frac{dJ_1}{dh} \right) - \frac{B+1}{2} \left(\frac{dJ_2}{dh} \right) \\ &= \frac{2h(2B-1)}{3} \left(\frac{dJ_0}{dh} \right) + \frac{B-6h-2}{3} \left(\frac{dJ_1}{dh} \right) \\ &= BJ_0 - \frac{5}{2}J_1 = \frac{J_0}{2}(2B - 5\Phi). \end{aligned}$$

□

Remark B.4 Since $M(0) = \frac{2}{3}(B-2)$ when $h=0$, we must choose $B < 2$ in order to have $M(h) < 0$ for any $h \geq 0$.

From Lemma B.2, the function $\Phi(h) = J_1(h)/J_0(h)$ satisfies the following Ricatti differential equation:

$$\frac{d\Phi}{dh} = \frac{1}{4h(4h+1)} \{5\Phi^2 + 4(2h-1)\Phi - 4h\}. \quad (\text{B.3})$$

Lemma B.5

$$\lim_{h \rightarrow \infty} \Phi(h) = +\infty.$$

Proof. Since $c(h) = O(h^{1/4})$, we have

$$J_0(h) = \int_0^{c(h)} \sqrt{2h + U^2 - U^4/2} dU \leq \sqrt{2h + \frac{1}{2}} \times c(h) = O(h^{3/4}).$$

On the other hand, letting $\tilde{c}(h) = O(h^{1/4})$ be the solution of $2h + U^2 - U^4/2 = h$, we have

$$J_1(h) \geq \int_1^{\tilde{c}(h)} U^2 \sqrt{h} dU = \frac{\tilde{c}^3 - 1}{3} \sqrt{h} = O(h^{5/4}).$$

Therefore

$$\Phi(h) = \frac{J_1(h)}{J_0(h)} \geq O(h^{1/2}) \rightarrow +\infty \quad (h \rightarrow \infty).$$

□

Now we give a proof of Proposition 4.4.

Proof. We show that the function $\Phi(h)$ has a positive minimum for $h \geq 0$. Since $\Phi(h)$ satisfies the Ricatti differential equation (B.3), the solution correspond to an invariant curve of the vector field

$$\dot{h} = 4h(4h + 1), \quad \dot{\Phi} = 5\Phi^2 + 4(2h - 1)\Phi - 4h,$$

that passes the point $(h, \Phi) = (0, 4/5)$. The above vector field has equilibrium points at $(0, 0)$ and $(0, 4/5)$, and the linearization matrix at $(0, 4/5)$ is $\begin{pmatrix} 4 & 0 \\ 12/5 & 4 \end{pmatrix}$, hence it is an unstable node. The vector field is such that it points downward on the half-line give by $\Phi = 0$ and $h > 0$, whereas upward on the half-line given by $\Phi = 4/5$ and $h > 0$. Therefore the asymptotic behavior of the solution orbit in the limit of $h \rightarrow \infty$ is either (i) it has a minimum and tends to $+\infty$ as $h \rightarrow \infty$, or (ii) it remains bounded from above as $h \rightarrow \infty$. However, the latter is not possible because of Lemma B.5, and thus there must be a minimum which is given by $\dot{\Phi} = 0$ or equivalently

$$h = -\frac{\Phi(5\Phi - 4)}{4(2\Phi - 1)}.$$

From the graph of this, we can easily see that the minimum Φ_0 is larger than $1/2$. Letting B_0 be $\frac{5}{2} \cdot \Phi_0$, hence $B_0 > 5/4$, we have that for any $B < B_0$

$$M(h) = \frac{1}{2}J_0(h)(2B - \Phi) \leq \frac{1}{2}(2B - 2B_0) = \frac{2}{3}(B - B_0) < 0.$$

Therefore, we obtain the desired conclusion by choosing $M_0 = (2/3) \cdot (B - B_0)$. This completes the proof of Proposition 4.4. \square

References

- [1] V. Afraimovich, V. Bykov, and L. Shilnikov, On structurally unstable attracting limit sets of Lorenz attractor type, *Trans. Moscow Math. Soc.* **44** (1983), 153–216.
- [2] V. Afraimovich, S.-N. Chow, W. Liu, Lorenz type attractors from codimension one bifurcation, *J. Dynam. Diff. Eq.* **7** (1995), 375–407.
- [3] M. Benedicks and L. Carleson, The dynamics of the Hénon maps, *Ann. Math.* **133** (1991), 1–25.
- [4] V. Bykov, The bifurcations of separatrix contours and chaos, *Physica* **D62** (1993), 290–299.
- [5] J. Carr, *Applications of Centre Manifold Theory*, Applied Math. Sciences Vol.35, 1981, Springer-Verlag.
- [6] X. Chen, Lorenz equations, I: Existence and nonexistence of homoclinic orbits, *SIAM J. Math. Anal.* **27** (1996), 1057–1069; *ibid.*, II: “Randomly” rotated homoclinic orbits and chaotic trajectories, *Disc. Cont. Dynam. Sys.* **2** (1996), 121–140; *ibid.*, III: Existence of hyperbolic sets, preprint.
- [7] B. Deng, The Shil’nikov problem, exponential expansion, strong λ -lemma, C^1 -linearization, and homoclinic bifurcation, *J. Diff. Eq.* **79** (1989), 189–231.

- [8] B. Deng, Constructing Lorenz type attractors through singular perturbations, *Intern. J. Bif. Chaos* **5** (1995), 1633–1642.
- [9] F. Dumortier, Techniques in the theory of local bifurcations: Blow-up, normal forms, nilpotent bifurcations, singular perturbations, in *Bifurcations and Periodic Orbits of Vector Fields* (ed. D.Schlomiuk), NATO ASI Series C, Vol. 408, 1993, Kluwer Academic Publisher, pp.19–73.
- [10] F. Dumortier and H. Kokubu, Chaotic dynamics in \mathbb{Z}_2 -equivariant unfoldings of codimension three singularities of vector fields in \mathbb{R}^3 , *Ergod. Th. & Dynam. Sys.* **20** (2000), 85–107.
- [11] F. Dumortier, H. Kokubu, and H. Oka, A degenerate singularity generating geometric Lorenz attractors, *Ergod. Th. & Dynam. Sys.* **15** (1995), 833–856.
- [12] F. Dumortier, P. Rodrigues, and R. Roussarie, *Germes of Diffeomorphisms in the Plane*, Lect. Notes Math., Vol. 902, 1981, Springer-Verlag.
- [13] Z. Galias and P. Zgliczyński, Computer assisted proof of chaos in the Lorenz equations, *Physica* **D115** (1998), 165–188.
- [14] J. Guckenheimer, A strange, strange attractor, in *The Hopf Bifurcation and Its Applications* (by J. Marsden and M. McCracken), 1976, Springer-Verlag, pp.368–381.
- [15] J. Guckenheimer and P. Holmes, *Nonlinear Oscillations, Dynamical Systems and Bifurcations of Vector Fields*, 1983, Springer-Verlag.
- [16] J. Guckenheimer and R. Williams, Structural stability of Lorenz attractors, *Publ. Math. I.H.E.S.* **50** (1979), 59–72.
- [17] S. P. Hastings and W. C. Troy, A shooting approach to chaos in the Lorenz equations, *J. Diff. Eq.* **127** (1996), 41–53.
- [18] M. Hénon, A two dimensional mapping with a strange attractor, *Commun. Math. Phys.* **50** (1976), 69–77.
- [19] M. Hénon and Y. Pomeau, Two strange attractors with a simple structure, in *Turbulence and Navier-Stokes equations*, Lect. Notes Math., Vol. 565, 1976, Springer-Verlag, pp. 29–68.
- [20] A. J. Homburg, Periodic attractors, strange attractors and hyperbolic dynamics near homoclinic orbits to saddle-focus equilibria, *Nonlinearity* **15** (2002), 1029–1050.
- [21] A. J. Homburg, H. Kokubu, and V. Naudot, Homoclinic doubling cascades, *Arch. Rat. Mech. Anal.* **160** (2001), 195–243.
- [22] A. J. Homburg and B. Krauskopf, Resonant homoclinic flip bifurcations, *J. Dynam. Diff. Eq.* **12** (2000), 807–850.
- [23] E. N. Lorenz, Deterministic nonperiodic flow, *J. Atmosph. Sci.* **20** (1963), 130–141.
- [24] S. Luzzatto and M. Viana, Positive Lyapunov exponents for Lorenz-like families with criticalities, in *Géométrie complexe et systèmes dynamiques (Orsay, 1995)*, Astérisque, No. 261, 2000, pp. 201–237; Lorenz attractors without continuous invariant foliations, in preparation.

- [25] K. Mischaikow, M. Mrozek and A. Szymczak, Chaos in the Lorenz equations: a computer assisted proof. III. Classical parameter values, *J. Diff. Eq.* **169** (2001), 17–56.
- [26] T. Oguro, Bifurcation of geometric Lorenz attractors from double homoclinic orbits (in Japanese), Master Thesis, Kyoto University, 2001.
- [27] H. Oka, Bifurcation of Lorenz-like attractors from a degenerate vector field singularity, in *Towards the Harnessing of Chaos*, (ed. M. Yamaguti), The Seventh TOYOTA Conference Proceedings, 1994, Elsevier, pp. 389–392.
- [28] C. Robinson, Homoclinic bifurcation to a transitive attractor of Lorenz type, *Nonlinearity* **2** (1989), 495–518; Homoclinic bifurcation to a transitive attractor of Lorenz type, II, *SIAM J. Math. Anal.* **23** (1992), 1255–1268.
- [29] O. E. Rössler, Continuous chaos — four prototype equations, in *Bifurcation theory and applications in scientific disciplines*, Ann. New York Acad. Sci., Vol. 316, New York Acad. Sci., New York, 1979, pp. 376–392.
- [30] R. Roussarie, Techniques in the theory of local bifurcations: Cyclicity and desingularization, in *Bifurcations and Periodic Orbits of Vector Fields* (ed. D. Schlomiuk), NATO ASI Series C, Vol. 408, 1993, Kluwer Academic Publisher, pp.348–382.
- [31] R. Roussarie, *Bifurcations of Planar Vector Fields and Hilbert’s Sixteenth Problem*, 1998, Birkhäuser.
- [32] M. Rychlik, Lorenz attractors through Šil’nikov-type bifurcation, Part I, *Ergod. Th. & Dynam. Sys.* **10** (1990), 93–109.
- [33] A. Shil’nikov, On bifurcations of a Lorenz-like attractor in the Shimizu-Morioka system, *Physica* **D62** (1992), 332–346.
- [34] A. Shil’nikov, L. Shil’nikov and D. Turaev, Normal forms and Lorenz attractors, *Intern. J. Bif. Chaos* **3** (1993), 1123–1139.
- [35] L. P. Shil’nikov, A case of the existence of a countable number of periodic motions, *Soviet Math. Dokl.* **6** (1965), 163–166.
- [36] T. Shimizu and N. Morioka, On the bifurcation of a symmetric limit cycle to an asymmetric one in a simple model, *Phys. Lett.* **A76** (1980), 201–204.
- [37] C. Sparrow, *The Lorenz Equations: Bifurcations, Chaos and Strange Attractors*, 1982, Springer-Verlag.
- [38] F. Takens, Partially hyperbolic fixed points, *Topology* **10** (1971), 133–147.
- [39] W. Tucker, The Lorenz attractor exists, *C. R. Acad. Sci. Paris, Série I*, **t.328** (1999), 1197–1202; more information, especially the codes can be found in <http://www.math.uu.se/~warwick>.
- [40] S. Ushiki, H. Oka, et H. Kokubu, Attracteurs étranges dans le déploiement d’une singularité dégénérée d’un champ de vecteurs invariant par translation, *C. R. Acad. Sci. Paris, Série I*, **t.298** (1984), 39–42.
- [41] M. Viana, What’s new on Lorenz strange attractors?, *Math. Intelligencer* **22** (2000), No.3, 6–19.

Figure Captions

Figure 1: The “standard” Lorenz attractor.

Figure 2: A singularly degenerate heteroclinic cycle.

Figure 3: Chaotic attractor of the Lorenz system at $r = 210$, $b = 8/3$ and $\sigma = 10$.

Figure 4: A chaotic attractor of Lorenz system (1.1) at $r = 185$.
Upper: (x, z) -plot; Lower: (x, y) -plot.

Figure 5: Chaotic attractor of the Rössler’s second system. (x, y) -plot.

Figure 6: A singularly degenerate heteroclinic cycle in the Lorenz system, $r = 1000$, $b = 0$ and $\sigma = 10$.

Figure 7: Sets W_{\pm} in Lemma 4.7.

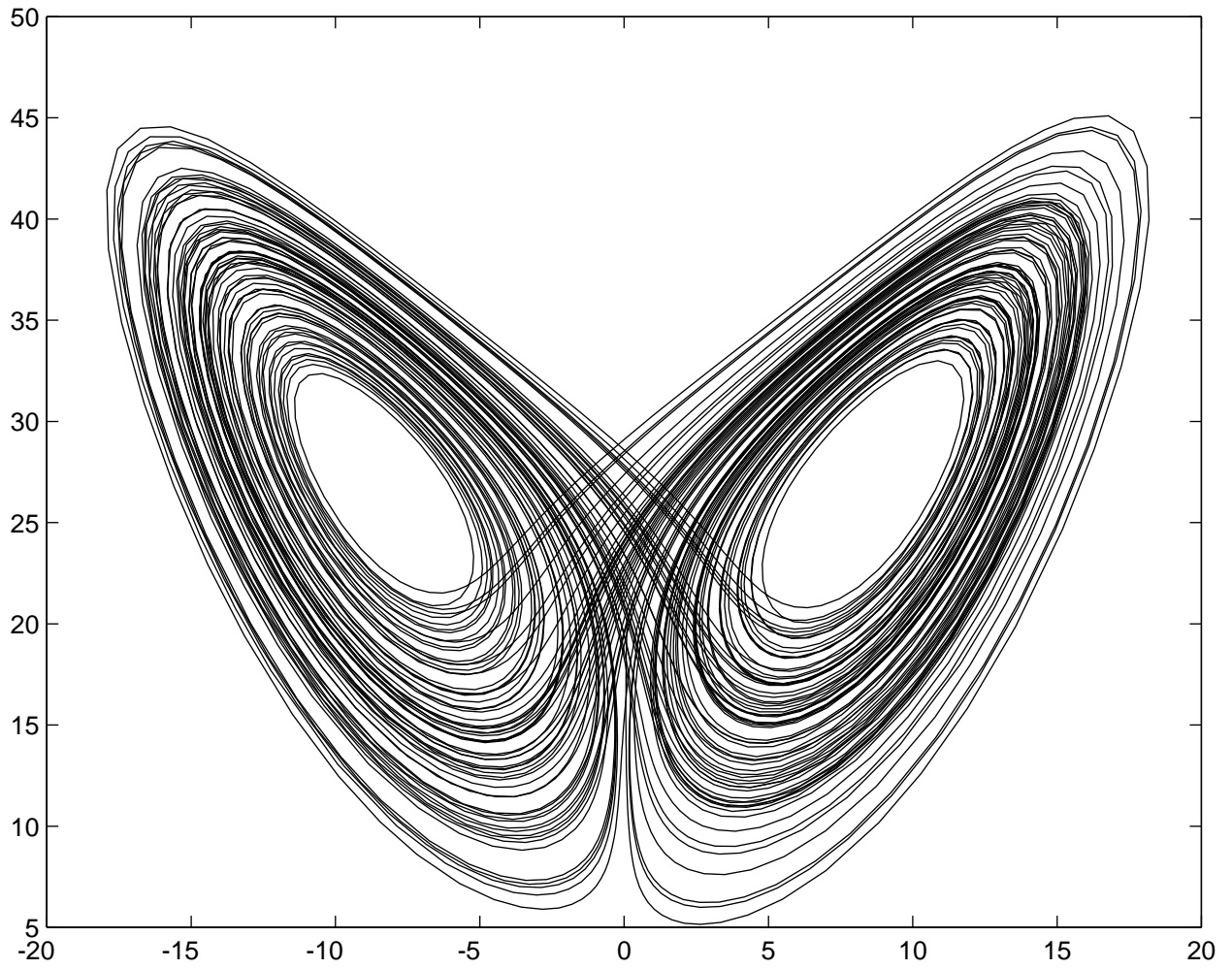


Figure 1: The “standard” Lorenz attractor.

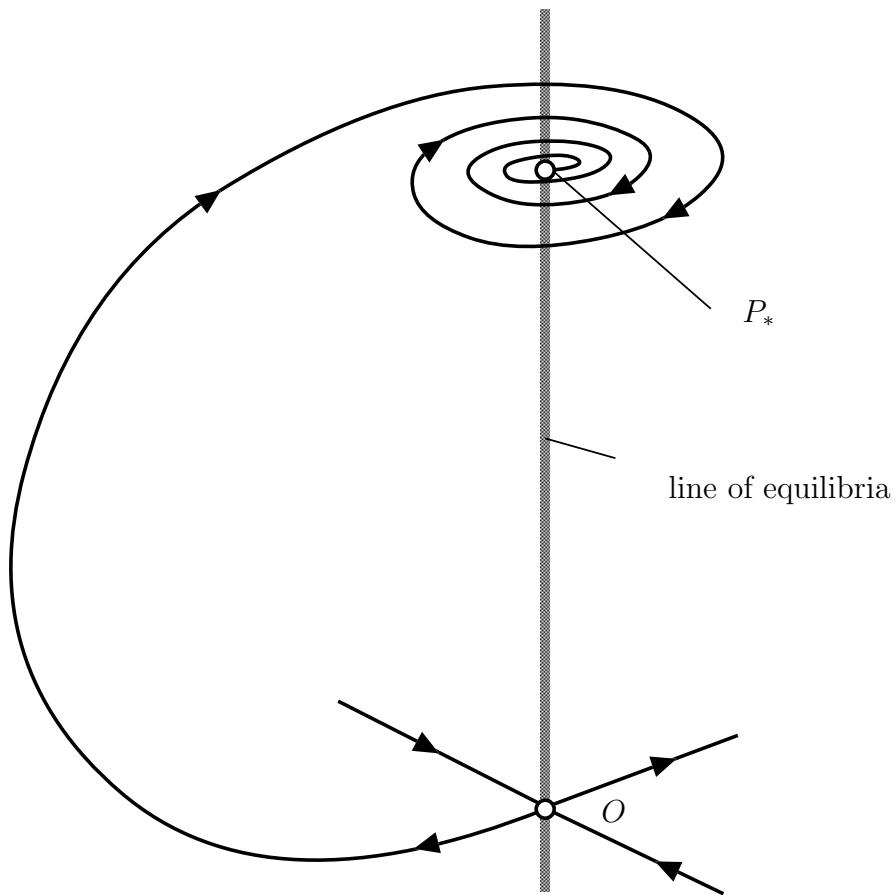


Figure 2: A singularly degenerate heteroclinic cycle.

An attractor in Lorenz equation; $r=210$

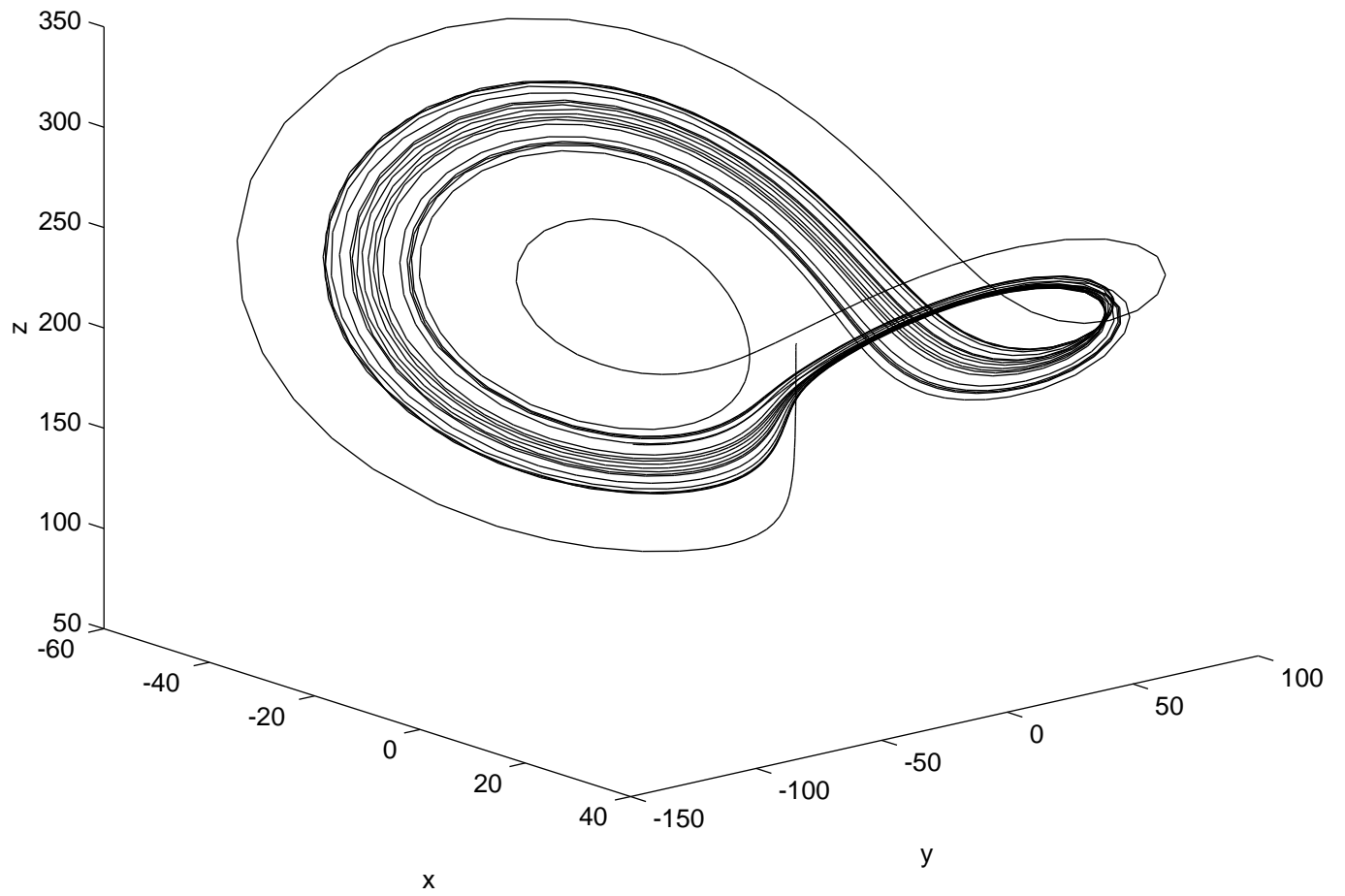


Figure 3: Chaotic attractor of the Lorenz system at $r = 210$, $b = 8/3$ and $\sigma = 10$.

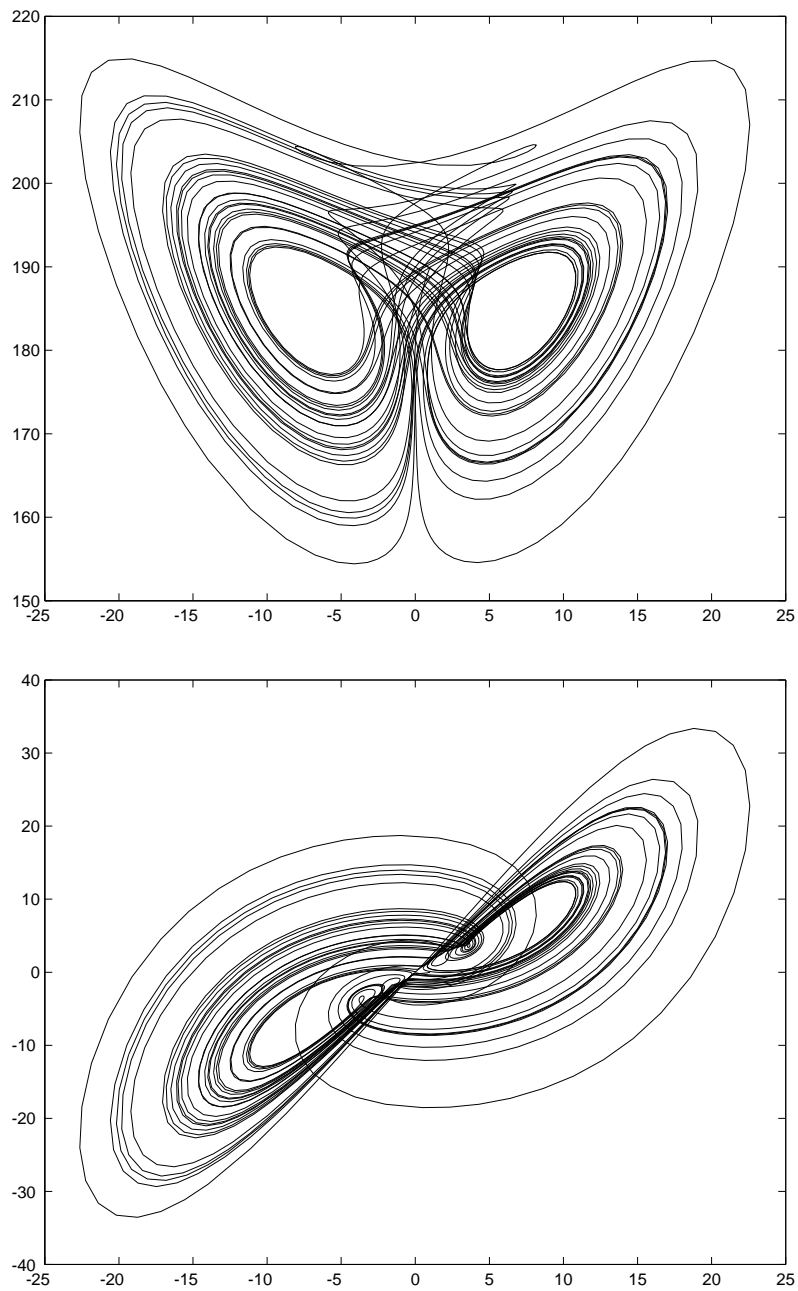


Figure 4: A chaotic attractor of Lorenz system (1.1) at $r = 185$.
Upper: (x, z) -plot; Lower: (x, y) -plot

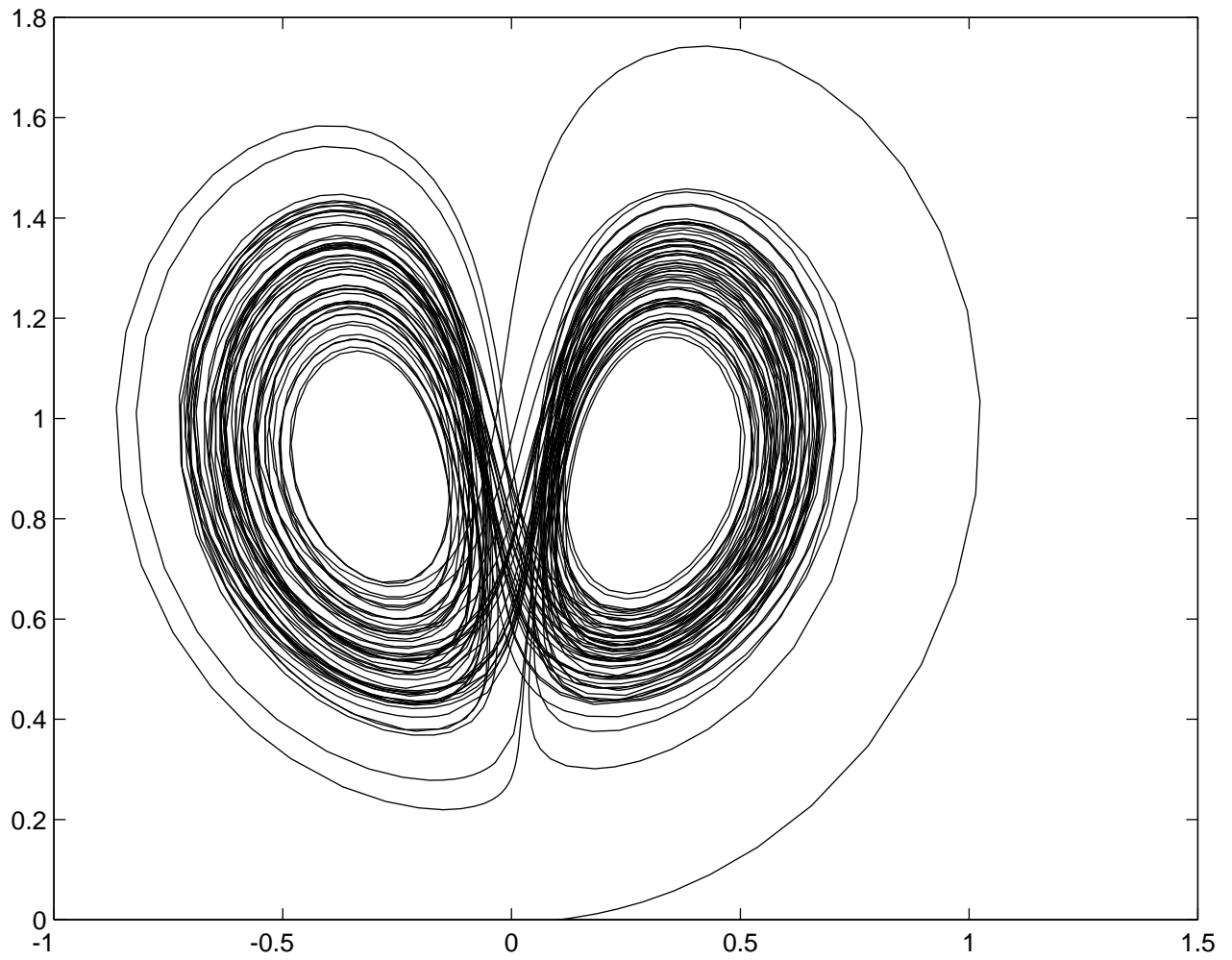


Figure 5: Chaotic attractor of the Rössler's second system. (x, y) -plot.

Singularly degenerate heteroclinic cycle in Lorenz equation; $r=1000$

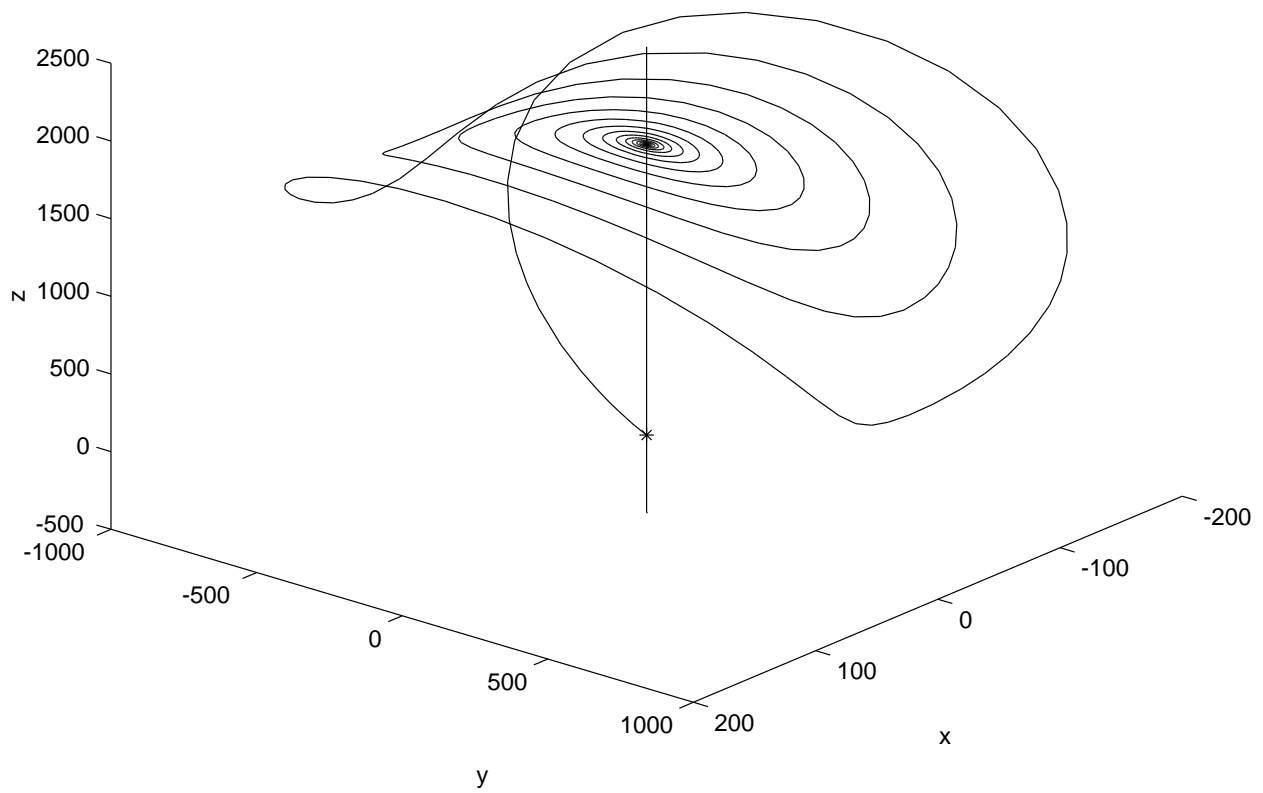


Figure 6: A singularly degenerate heteroclinic cycle in the Lorenz system, $r = 1000$, $b = 0$ and $\sigma = 10$.

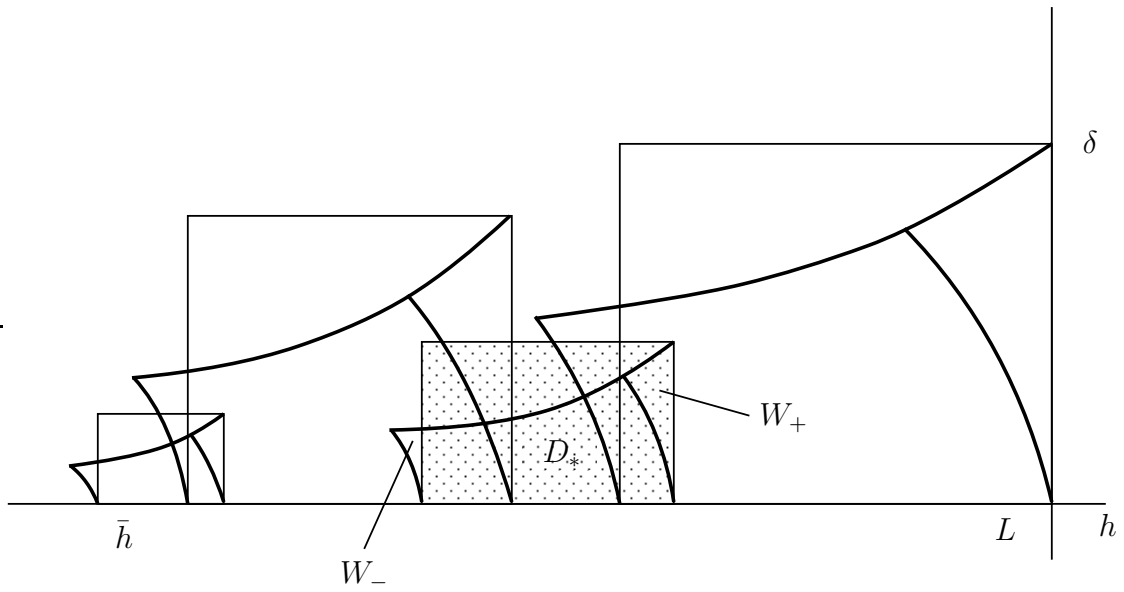


Figure 7: Sets W_{\pm} in Lemma 4.7